arXiv:2003.05554v2 [stat.ML] 20 Jan 2021

GENERAL LINEAR-TIME INFERENCE FOR GAUSSIAN PROCESSES ON ONE DIMENSION

Jackson Loper
Data Science Institute
Columbia University
New York, New York 10027
jl5116@columbia.edu

David Blei
Data Science Institute
Columbia University
New York, New York 10027

John P. Cunningham
Department of Neuroscience
The Studebaker Building, MC 8765
615 West 131st Street, 6th floor
New York NY 10027

Liam Paninski
Department of Neuroscience
The Studebaker Building, MC 8765
615 West 131st Street, 6th floor
New York NY 10027

May 24, 2022

ABSTRACT

Gaussian Processes (GPs) provide powerful probabilistic frameworks for interpolation, forecasting, and smoothing, but have been hampered by computational scaling issues. Here we investigate data sampled on one dimension (e.g., a scalar or vector time series sampled at arbitrarily-spaced intervals), for which state-space models are popular due to their linearly-scaling computational costs. It has long been conjectured that state-space models are general, able to approximate any one-dimensional kernel. We provide the first general proof of this conjecture, showing that any stationary GP on one dimension with vector-valued observations governed by a Lebesgue-integrable continuous kernel can be approximated to any desired precision using a specifically-chosen state-space model: the Latent Exponentially Generated (LEG) family. This new family offers several advantages compared to the general state-space model: it is always stable (no unbounded growth), the covariance can be computed in closed form, and its parameter space is unconstrained (allowing straightforward estimation via gradient descent). The theorem's proof also draws connections to Spectral Mixture Kernels, providing insight about this popular family of kernels. We develop parallelized algorithms for performing inference and learning in the LEG model, test the algorithm on real and synthetic data, and demonstrate scaling to datasets with billions of samples.

1 Introduction

Gaussian Process (GP) methods are a powerful and expressive class of nonparametric techniques for interpolation, forecasting, and smoothing. However, this expressiveness comes at a cost: if implemented naively, inference in a GP given m observed data points will require $O(m^3)$ operations. A large body of work has devised various means to circumvent this cubic run-time; briefly, this literature can be broken down into several threads. A first approach is to attempt to perform exact inference without imposing any restrictions on the covariance kernel, using careful numerical methods typically including preconditioned conjugate gradients [Cutajar et al., 2016]. Wang et al. [2019] represents the state of the art: inference and learning can be performed on $\sim 10^6$ datapoints on an 8-GPU machine and a few days of processing time. A second approach searches for good approximations to the posterior (e.g., low-rank approximations to the posterior covariance) that do not rely on special properties of the covariance kernel. Some well-known examples of this approach include [Quiñonero-Candela and Rasmussen, 2005, Snelson and Ghahramani, 2007, Hensman et al., 2013, Low et al., 2015, De G. Matthews et al., 2017]. In a third approach, several techniques exploit special kernel structure. Examples include matrices with Kronecker product structure [Gilboa et al., 2013], Toeplitz structure [Zhang et al.,

2005, Cunningham et al., 2008], matrices that can be well-approximated with hierarchical factorizations [Ambikasaran et al., 2015], or matrices which are sufficiently smooth to allow for interpolation-based approximations [Wilson and Nickisch, 2015].

When the GP has one-dimensional input, one popular method for scaling learning and inference is to approximate the GP with some form of Gaussian hidden Markov model (that is, a state-space model) [Reinsel, 2003, Mergner, 2009, Cheung et al., 2010, Brockwell and Davis, 2013]. This model class has considerable virtue: it is a particular case of a GP, it includes popular models like the auto-regressive moving average process (ARMA, when on an evenly spaced grid), and perhaps most importantly it admits linear-time $O(m)$ inference via message passing.

It has long been conjectured that state-space models are not only fast, but general. In several special cases it has been shown that state-space models provide arbitarily-good approximations of specific covariance kernels [Karvonen and Sarkkä, 2016, Benavoli and Zaffalon, 2016, Särkkä and Solin, 2019]. Discrete-time processes on a finite interval can also be approximated this way [Lindgren et al., 2011]. The idea is simple: by taking a sufficiently high-dimensional latent space, one can produce processes whose observed covariance is quite intricate. Practically, [Gilboa et al., 2013] suggests it is straightforward to learn many GP models using state-space techniques.

However, no proof of this conjecture yet existed. Karvonen and Sarkkä [2016] provide a good example of the types of results that have been achieved up until now. This paper develops theoretical tools for proving ways that Gaussian Process models can be approximated by state-space models. These tools represented a promising advance from what came before, insofar as they can be applied to arbitrary kernels. These tools allow one to transform problems of kernel approximation into more elegant proofs about Taylor series convergence. However, they do have some disadvantages. First, the proofs only show convergence for a compact subset of the Fourier transform of the kernels; thus the approximations might have arbitrarily poor high-frequency behavior. Second, the methods only apply to the case $n = 1$: they do not apply if one measures a vector of observations at each time-point.

Here we present a new theorem which lays the "generality" question to rest for time-series data with vector-valued observations. It is based on a connection between state-space models and Spectral Mixture kernels [Wilson and Adams, 2013]. The new theorem shows that that any stationary GP on one dimension with vector-valued observations and a Lebesgue-integrable continuous kernel can be uniformly approximated by a state-space model. In particular: for any positive-definite Lebesgue-integrable continuous kernel and any value of ε, one can find a state-space model so that all covariances are within ε of the target kernel. Along the way, we also proved a similar generality result for Spectral Mixture kernels of the form $\Sigma : \mathbb{R} \to \mathbb{R}^{n\times n}$ (this result was already known for the case $n = 1$, we generalized the proof to the case $n > 1$).

To prove this theorem, we developed a convenient family of Gaussian hidden Markov models on one dimension: the Latent Exponentially Generated (LEG) process. This model has several advantages over the general state-space models: its covariance can be computed in closed form, it is stable (with no unbounded growth), and its parameter space is unconstrained (allowing for simple gradient descent methods to be applied to learn the model parameters). The LEG model generalizes the Celerite family of Gaussian Processes [Foreman-Mackey et al., 2017] to allow more model flexibility and permit vector-valued observations. Unlike some popular state-space models such as the ARMA, LEG processes do not require that the observations are equally spaced. LEG kernels have an intersection with spectral mixture kernels [Wilson and Adams, 2013], which enables a proof that these LEG kernels can approximate any integrable continuous kernel. Thus LEG models are general: our main mathematical result is to prove that for any stationary Gaussian Process x on one dimension with integrable continuous covariance, for any ε, the covariance of x can be matched within ε by a LEG covariance kernel. Finally, inference for the LEG processes can be parallelized efficiently via a technique known as Cyclic Reduction [Sweet, 1974], leading to significant runtime improvements.

To summarize, this paper contains three contributions. First, it is shown for the first time that any vector-valued GP on one dimension with a stationary integrable kernel can be approximated to arbitrary accuracy by a state-space model. Second, an unconstrained parameterization for state-space models is developed (the LEG family). Finally, based on that parameterization, this paper introduces an open-source, parallel-hardware, linear-time package for learning, interpolating, and smoothing vector-valued continuous-time state-space models with irregularly-timed observations.

The remainder of this paper defines the LEG family, derives its essential properties and generality, and finally empirically backs up these claims across real and synthetic data. In particular, we show that the LEG family enables inference on datasets with billions of samples with runtimes that scale in minutes, not days.

2 The LEG kernel

A Gaussian Process on one dimension is a random function $x : \mathbb{R} \to \mathbb{R}^n$ such that for any finite collections of times $t_1, t_2 \cdots t_m$ the distribution of $(x(t_1), \cdots x(t_m)) \in \mathbb{R}^{m\times n}$ is jointly Gaussian. The covariance kernel of x is a matrix-

valued function defined by $\Sigma(s,t) = \mathrm{Cov}(x(s), x(t)) \in \mathbb{R}^{n\times n}$. A process is said to be stationary if $\Sigma(s,t) = C(s-t)$ for some matrix-valued function C and $\mathbb{E}[x(t)]$ is the same for all values of t. In this case we write τ for the time-lag $t-s$, i.e $C = C(\tau)$. For clarity of exposition, what follows assumes stationarity and zero mean; generalizations are discussed in Section 5.

Some stationary Gaussian Processes are also *linear state-space models*. For the purposes of this article, we will say a process is a state-space model if there is a Markovian Gaussian Process $z : \mathbb{R} \to \mathbb{R}^\ell$ and at each timepoint t we independently sample $x(t) \sim \mathcal{N}(Bz(t), \Lambda\Lambda^\top)$ with some matrices B, Λ. The process z is called the "latent" process: it is used to define a distribution on the observations, x, but it may not actually refer to any observable property of the physical world. The matrices B, Λ are referred to as the "observation model."

This paper began with the following question: can all stationary Gaussian Processes be approximated arbitrarily well with some state-space model?

To answer this question, we found it convenient to design a family of linear-state space models which we call the "Latent Exponentially-Generated" family. Among other advantages, it is easier to compute marginal covariances for members of this family, which enabled simpler analyses. In this section we will define this family. To do so, we will start by defining a latent Markovian GP, then we will define the observation model. Taken together these objects will form the LEG family of state-space models.

In designing a state-space model, a classic choice for the latent Markovian GP is given by the linear Langevin equations [Coffey et al., 2004], i.e. processes defined by $z(t) = z(0) + \int_0^t (-Gz(s)ds + \sigma dw(s))$, where w is an ℓ-dimensional Brownian motion, and G, σ are square matrices. To ensure this process doesn't grow without bound, we need the real part of the eigenvalues of G to be positive. Guaranteeing this nontrivial constraint is challenging [Buesing et al., 2012, Choudhary et al., 2019]. To remedy this problem we developed a closely-related family of models which are always stable and stationary:

Definition 1. Let $z(0) \sim \mathcal{N}(0, I)$, let w denote a Brownian motion, let N, R be any $\ell \times \ell$ matrices, and let $G = NN^\top + R - R^\top$. Let z satisfy $z(t) = z(0) + \int_0^t \left(-\frac{1}{2}Gz(s)ds + Ndw(s)\right)$. Then we will say z is a Purely Exponentially Generated process, $z \sim \mathrm{PEG}(N, R)$.

Not only is this family automatically stable, it also has another advantage: the covariance kernel is easy to compute. The covariance kernel for linear Langevin models usually involves an integral [Vatiwutipong and Phewchean, 2019], but for PEG models we can compute this integral in closed form:

Lemma 1. *$z \sim \mathrm{PEG}(N, R)$ is stationary, with covariance kernel given by*

$$C_{\mathrm{PEG}}(\tau; N, R) \triangleq \exp\left(-\frac{\tau}{2}\left(NN^\top + R - R^\top\right)\right)$$

for $\tau \geq 0$ (for $\tau < 0$ it may readily be computed that $C(\tau)$ must be given by $C(-\tau)^\top$).

Proof: This and every proof will be deferred to the supplement.

The matrices N, R can be interpreted intuitively. The positive definite diffusion $NN^\top$ controls the predictability of the process: when an eigenvalue of $NN^\top$ becomes larger, the process z becomes less predictable along the direction of the corresponding eigenvector. The antisymmetric $R - R^\top$ term affects the process by applying an infinitesimal deterministic rotation at each point in time. The eigenvalues of $R - R^\top$ are purely imaginary, and when they are large they lead to strong rapid oscillations in the process, while the eigenvectors control how these oscillations are mixed across the dimensions of z. As an illustration, Figure 1 shows the first dimension of samples from an $\ell = 2$ dimensional PEG process with various values of N, R.

We now turn to the observed process:

Definition 2. Let $z \sim \mathrm{PEG}(N, R)$. Fix any $n \times \ell$ matrix B and any $n \times n$ matrix Λ. For each t independently, define the conditional observation model: $x(t)|z(t) \sim \mathcal{N}(Bz(t), \Lambda\Lambda^\top)$. We define a **Latent Exponentially Generated (LEG)** process to be the Gaussian Process $x : \mathbb{R} \to \mathbb{R}^n$ generated by a PEG prior and the above observation model. We write $x \sim \mathrm{LEG}(N, R, B, \Lambda)$. X has a LEG kernel: $C_{\mathrm{LEG}}(\tau; N, R, B, \Lambda) \triangleq B\left(C_{\mathrm{PEG}}(\tau; N, R)\right)B^\top + \delta_{\tau=0}\Lambda\Lambda^\top$. Here δ is the indicator function. We will refer to the latent dimension ℓ as the **rank** of the LEG kernel.

The LEG sub-family of state-space models has two advantages over general continuous-time state-space models. First, to compute covariances for Langevin equations, we need to compute integrals of matrix exponentials, but LEG models require only a single matrix-exponential computation. In particular, computing $C_{\mathrm{PEG}}(\tau; N, R)$ for m different values of τ requires a single $\ell \times \ell$ matrix diagonalization followed by the computation of ℓ scalar exponentials for each τ, i.e. $O(\ell^3 + m\ell)$. Second, the set of valid parameters in Langevin-based state-space models is difficult to characterize and

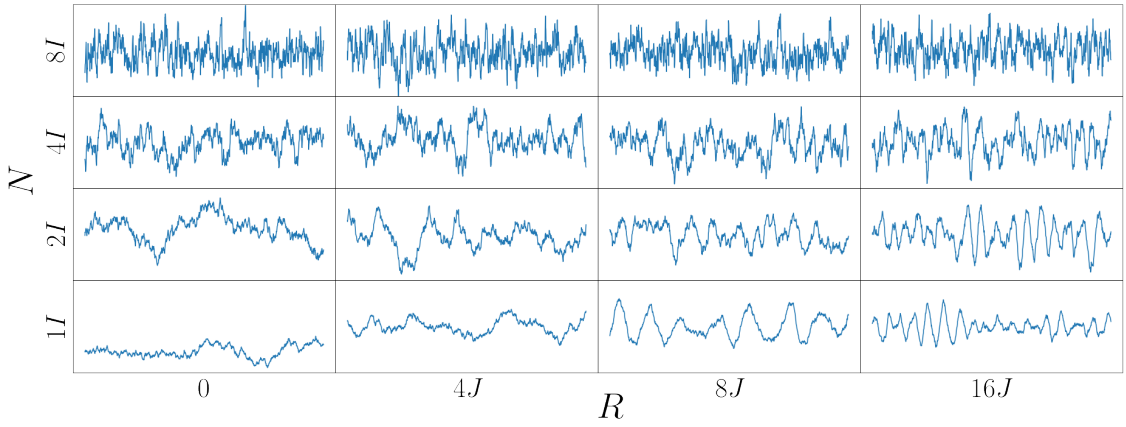

Figure 1: **PEG process samples**. The plots above show representative samples from the model $\mathrm{PEG}(N, R)$ as we vary N and R. Here we consider rank-2 PEG models (only one element of the 2d vector is plotted), so N, R are both 2×2 matrices. We vary N by taking it to be various multiples of the identity. We vary R by taking various multiples of J, the antisymmetric 2×2 matrix with zeros on the diagonal and ± 1 on the off-diagonal. In this simple rank-2 case, increasing N leads to a less predictable process and increasing R leads to faster oscillations.

enforce (involving the real part of eigenvalues of a matrix) whereas the parameter-space for LEG models is entirely unconstrained; this allows us to apply unconstrained gradient-descent techniques to fit these models.

3 Generality of the LEG family

We here show that *any* stationary Lebesgue-integrable continuous kernel can be approximated to arbitrary accuracy with a LEG model, i.e. any Gaussian Process with such a covariance can be accurately modeled using a member of the LEG family. We achieve this in two steps:

1. We show that the family of Cauchy-based Spectral Mixture kernels is a strict subset of the LEG family.
2. We prove that the family of Cauchy-based Spectral Mixture kernels can approximate any stationary Lebesgue-integrable continuous kernel. This fact is readily achieved (via Bochner's theorem) for processes of the form $x : \mathbb{R}^d \to \mathbb{R}$; here we prove the same result for the more general case, processes $x : \mathbb{R} \to \mathbb{R}^n$ $n = 1$. This generalization requires some technical detail, because it involves the matrix-valued spectra of covariances for timeseries with vector-valued observations.

Together, these two results show us that the LEG family – a linear-time state-space model – can approximate the kernels we want to approximate. Along the way, we will also see that another popular family of kernels – known as the "Celerite" family – also enjoys this guarantee.

3.1 Three families of kernels

Here we will discuss how the LEG family relates to two families of kernels from the literature.

The Spectral Mixture (SM) kernels comprise the first family of kernels we will consider. Recall that if a kernel for a Gaussian time series is stationary and continuous, it is guaranteed to have a spectrum [Bhatia, 2015]: a unique matrix-valued measure F such that $C(\tau) = \int e^{-i\tau\omega} dF(\omega)$. SM kernels approximate kernels directly through their spectra. For the purposes of this article we will define SM kernels as follows:

Definition 3. Let K denote a probability density on $\mathbb{R}$, let $b_1, b_2 \cdots b_\ell \in \mathbb{C}^n$, let $\mu \in \mathbb{R}^\ell$, and let $\gamma > 0$. The **Spectral Mixture** kernel, $C_{\mathrm{SM}}(t; K, b, \mu, \gamma)$, is given by $\sum_{k=1}^{\ell} \int e^{-i\xi x} b_k b_k^* \gamma K(\gamma(\xi - \mu_k)) d\xi$. Here b_k^* denote the conjugate transpose of b. We will say that C is **based on** K, since its spectrum is a sum of scaled and shifted versions of K.

Spectral Mixtures were first introduced in machine learning by Wilson and Adams [2013], where it was noted that any kernel which is the covariance of a weakly stationary mean square continuous random process $X : \mathbb{R} \to \mathbb{R}$ (or indeed $X : \mathbb{R}^n \to \mathbb{R}$) can be well-approximated using SM kernels. Unfortunately, that result does not hold for

our case, i.e. kernels for processes of the form $X : \mathbb{R} \to \mathbb{R}^n$; in this situation the spectrum of the kernel becomes a complex-matrix-valued measure (instead of an ordinary probability measure), necessitating a generalization (see Corollary 1, below).

Celerite kernels comprise the second family we consider, introduced by Foreman-Mackey et al. [2017]. These kernels are designed only for the case $n = 1$. They are built by linear combinations of kernels called "Celerite terms." These terms take the form

$$C(\tau; a, b, c, d) = a \exp(-c|\tau|) \cos(d|\tau|) + b \exp(-c|\tau|) \sin(d|\tau|);$$

Note that such terms are not always valid kernels, i.e. there are parameters a, b, c, d such that $C(\cdot; a, b, c, d)$ is not the kernel of *any* Gaussian Process. If a Celerite term is the kernel of a Gaussian Process, it is said to be "positive-definite." See [Foreman-Mackey et al., 2017] for background and full details.

Below we summarize the relationship between these three families of kernels:

Lemma 2 (SM kernels, Celerite kernels, LEG kernels)**.**

1. *Every Cauchy-based real-valued SM kernel $C_{\mathrm{SM}} : \mathbb{R} \to \mathbb{R}$ is also a Celerite kernel.*
2. *Every positive-definite Celerite term is also a LEG kernel.*
3. *Every Cauchy-based real-valued SM kernel $C_{\mathrm{SM}} : \mathbb{R} \to \mathbb{R}^{n \times n}$ is also a LEG kernel.*

The most key takeaway from this Lemma is simple: the Celerite family and the LEG family are supersets of the Cauchy-based SM family. Thus, to show that the Celerite family and the LEG family can approximate a kernel Σ, it suffices to show that the Cauchy-based SM family can approximate Σ.

3.2 Cauchy-based SM kernels are good approximators ($n = 1$)

It is well-known that the Cauchy-based Spectral Mixture family can approximate kernels of the form $\Sigma : \mathbb{R}^d \to \mathbb{R}$ (similar results for Spectral Mixtures based on other distributions have also been proven, though they are out of the scope of this paper). We are interested in kernels of the form $\Sigma : \mathbb{R} \to \mathbb{R}^{n \times n}$. To lay the groundwork for thinking about this case, we will first sketch the proof for the simplest case: kernels of the form $\mathbb{R} \to \mathbb{R}$.

Let $\Sigma : \mathbb{R} \to \mathbb{R}$ denote the covariance of a stationary Gaussian Process. Assume Σ is continuous and $\int |\Sigma(\tau)| d\tau < \infty$. Our task is to show that for any target error tolerance ε, we can find some Cauchy-based SM kernel C_{SM} so that $|C_{\mathrm{SM}}(\tau) - \Sigma(\tau)| < \varepsilon$ for every τ. We proceed in three steps:

Go to the spectral domain. Take the Fourier transform to obtain spectrum of the kernel. There are several different conventions of the Fourier transform, but in this paper we will say $\tilde{M}$ is the spectrum of Σ when

$$\Sigma(\tau) = \int \exp(-i\tau\omega) \tilde{M}(\omega) d\omega.$$

Bochner's theorem guarantees that $\tilde{M}$ is non-negative and $\Sigma(0) < \infty$ guarantees that M is integrable. It follows that we can write $\tilde{M}(\omega) = f(\omega)M$ where M is a normalizing constant and f is a probability density.

Kernel density approximation. In this Fourier domain, we can then use the machinery from kernel density estimation to show that we can get a good approximation to f by taking a mixture of Cauchy distributions. Specifically, let $\mu_1, \mu_2, \cdots \mu_\ell$ i.i.d $\sim f$, let $K(\omega)$ denote the Cauchy density and approximate

$$\tilde{M}(\omega) \approx \times \frac{1}{\ell} \sum_{k=1}^{\ell} \gamma K(\gamma(\omega - \mu_k)) M.$$

The usual kernel density arguments can be used to demonstrate that the approximation error becomes arbitrarily small as ℓ becomes sufficiently high (as long as γ is scaled carefully as $\ell \to \infty$).

Return to the temporal domain. The approximation in the spectral domain leads to an approximation in the temporal domain:

$$\Sigma(\tau) \approx \int \exp(-i\tau\omega) M \frac{1}{n} \sum_{k}^{\ell} \gamma K(\gamma(\omega - \mu_k)) d\omega = C_{\mathrm{SM}}(\tau; K, M, \mu, \gamma).$$

Since the approximation error in the spectral domain was small, the approximation error in the kernel will also be small (this argument can be made rigorous, but here we are only giving a rough sketch).

3.3 Cauchy-based SM kernels are good approximators ($n > 1$)

Now let us turn from the case $n = 1$ (which was already well-understood) to the new case: $n > 1$. Thus our target kernel is now a matrix-valued function of the form $\Sigma : \mathbb{R} \to \mathbb{R}^{n \times n}$. We follow the same steps, but there are several difficulties that must be overcome.

Go to the (matrix-valued) spectral domain. Taking the fourier transform of each entry of the matrix Σ, we obtain an overall matrix-valued spectrum, $\tilde{M}$:

$$\Sigma_{ij}(\tau) = \int \exp(-i\tau\omega)\tilde{M}_{ij}(\omega)d\omega.$$

Bochner's theorem no longer applies – in fact, $\tilde{M}_{ij}(\omega)$ is now complex-valued. However, there is a natural generalization of Bochner's theorem to thise case: for each ω it can be shown that $\tilde{M}(\omega)$ is a Hermitian nonnegative-definite matrix. The trace of these matrices can then be used to construct a density f, similar to the density we used for the the case $n = 1$. Specifically, we decompose $\tilde{M}$ as

$$\tilde{M}_{ij}(\omega) = f(\omega)M_{ij}(\omega),$$

where $f : \mathbb{R} \to \mathbb{R}^+$ is a probability density and M is a matrix-valued function such that $M(\omega)$ is Hermitian, nonnegative-definite, and having constant trace over all ω.

Weighted kernel density approximation. As before, we draw samples $\mu_1, \mu_2 \cdots \mu_\ell$ i.i.d $\sim f$. We then approximate

$$\tilde{M}_{ij}(\omega) \approx \frac{1}{\ell}\sum_{k=1}^{\ell} \gamma K(\gamma((\omega - \mu_k)))M_{ij}(\omega).$$

Note that the object M is a function of ω. By contrast, we recall that in the $n = 1$ case the object M was merely a fixed, scalar normalization constant. Due to this new dependence, the methods we used for the $n = 1$ case no longer apply. However, we can show that M is bounded. Inspired by this, we developed Theorem 1, below, which allows us to argue that the approximation error can indeed be made arbitrarily small in this situation.

Return to the temporal domain. The spectral approximation leads to an approximation in the temporal domain:

$$\Sigma_{ij}(\tau) \approx \int e^{-i\tau\omega}\frac{1}{\ell}\sum_{k=1}^{\ell} \gamma K(\gamma((\omega - \mu_k)))M_{ij}(\omega)d\omega. \tag{1}$$

Here we find another difference. The formula above cannot be *directly expressed as a spectral mixture kernel*. Why not? Examining our definition of spectral mixture kernels, we find that each component of the spectral mixture kernel involves an outer product of the form $b_k b_k^*$, i.e. a matrix of *rank 1*. Indeed, each mixture component is a kernel $C : \mathbb{R} \to \mathbb{R}^{n \times n}$ such that the matrix $C(\tau)$ is rank 1 for each τ. On the other hand, the formula in Equation 1 is written as a sum over ℓ matrices – and each of these matrices may well be full-rank ($M(\omega)$ may be full-rank).

To complete the story, we use the positive-definiteness of M to obtain eigendecompositions of the form $M(\omega_{k_1}) = \frac{1}{n}\sum_{k_2} b_{k_1 k_2} b_{k_1,k_2}^*$. This decomposition then allows us to write

$$\Sigma_{ij}(\tau) \approx \int e^{-i\tau\omega}\frac{1}{\ell \times n}\sum_{k_1=1}^{\ell}\sum_{k_2=1}^{n} \gamma K(\gamma((\omega - \mu_k)))b_{k_1 k_2} b_{k_1 k_2}^* d\omega.$$

Now we have a double sum over rank-1 terms; so we can express this as a spectral mixture kernel with $\ell \times n$ components. To do so, we let

$$\tilde{\mu} = \overbrace{\mu_1, \mu_1, \mu_1 \cdots \mu_1}^{n \text{ copies}}, \overbrace{\mu_2, \cdots \mu_2}^{n \text{ copies}}, \cdots \overbrace{\mu_\ell, \cdots \mu_\ell}^{n \text{ copies}}.$$

This $\tilde{\mu}$ allows us to reflect the fact that for every $k_1 \in \{1 \cdots \ell\}$ we have n different components, and all of those components actually share the same center, μ_{k_1}. Using $\tilde{\mu}$, we can write down our approximation as a spectral mixture:

$$\int e^{-i\tau\omega}\frac{1}{\ell \times n}\sum_{k_1=1}^{\ell}\sum_{k_2=1}^{n} \gamma K(\gamma((\omega - \mu_k)))b_{k_1 k_2} b_{k_1 k_2}^* d\omega = C_{\text{SM}}(\tau, K, b, \tilde{\mu}, \gamma),$$

We can thus argue that Σ can be approximated arbitrarily well by a Cauchy-based spectral mixture kernel with $n \times \ell$ components.

3.4 Formal statements

So far we have given only rough sketches for illustrative purposes. Let us now make these arguments rigorous. All proofs are deferred to the supplement, but here we will state the essential theorems. We begin by establishing a theorem for weighted kernel density estimation; this is necessary for the "weighted kernel density approximation" step, above.

Theorem 1 (Total variation convergence for weighted kernel density estimation)**.** *Let K, p denote bounded densities on $\mathbb{R}^d$. Let $g : \mathbb{R}^d \to [-M, M]$. Let $\gamma_\ell = \ell^{1/2d}$. Let $\mu_1, \mu_2 \cdots \sim p$, independently. For each $\ell \in 1, 2, \cdots$, define $h_\ell(\xi) = \frac{1}{\ell} \sum_{k=1}^{\ell} g(\mu_k)\gamma_\ell^d K(\gamma_\ell(\xi - \mu_k))$. Then*

$$\mathbb{P}\left(\lim_{\ell\to\infty} \int |h_\ell(\xi) - p(\xi)g(\xi)|d\xi = 0\right) = 1.$$

Once this theorem is in place, the result follows easily:

Corollary 1 (Flexibility of Spectral Mixture kernels)**.** *Fix K, a bounded probability density on $\mathbb{R}^n$, $\varepsilon > 0$, and any Lebesgue-integrable continuous positive definite[1] stationary kernel $\Sigma : \mathbb{R} \to \mathbb{C}^{n\times n}$. There exists a real valued kernel $C = C_{\mathrm{SM}}(K, b, \mu, \gamma)$ such that the spectral norm of $C(\tau) - \Sigma(\tau)$ is at most ε for every $\tau \in \mathbb{R}$.*

This corollary, together with Lemma 2, leads to the main mathematical result of this paper: LEG models enjoy the same flexibility guarantee.

Theorem 2 (Flexibility of LEG and Celerite kernels)**.** *For every $\varepsilon > 0$ and every Lebesgue-integrable continuous positive definite stationary kernel $\Sigma : \mathbb{R} \to \mathbb{R}^{n\times n}$ there exists a Celerite kernel C such that the spectral norm of $C(\tau) - \Sigma(\tau)$ is at most ε for every $\tau > 0$. Moreover, there exists a LEG kernel with the same guarantee.*

Note that there is no particular reason that we focused on the spectral norm of the matrices $C(\tau), \Sigma(\tau)$. Most matrix norms are topologically equivalent. For example, we could equivalently have showed that we can find a LEG kernel which guarantees $|C_{ij}(\tau) - \Sigma_{ij}(\tau)| \leq \varepsilon$ for all τ, i, j.

In conclusion, we have proven that any stationary Gaussian Process on one dimension can be well approximated using state-space models – in particular, using LEG processes. Thus we see that approximate inference for any stationary Gaussian Processes on one dimension at any desired level of accuracy requires computational effort that scales linearly with the number of observations.

4 The `leggps` package for fast state-space modeling

The LEG family is just a special family of state-space models, and there are some existing packages for working with sate-space models. Unfortunately – perhaps because of difficulties with previous parameterizations for state-space models – we were unable to find a package which took advantage of GPUs and also "just worked" for learning, interpolating, and smoothing vector-valued state-space models on irregularly-spaced data. The closest candidate we could find was the `GaussianHMM` class in the `pyro` package, which uses fast parallel algorithms based on associative scans [Särkkä and García-Fernández, 2019]; however, this package lacked some important features, such as the computation of posterior variances. In the interest of completeness, we constructed the `leggps` package as a modern tool for learning, smoothing, forecasting, and interpolating with continuous-time state-space models. Exact linear-time algorithms are given in the supplement. TensorFlow2-based Python code, tutorial notebooks, and API documentation can be found at `https://github.com/jacksonloper/leg-gps`.

Our goals in constructing this package were threefold.

4.1 No hand-tuning

This was straightforward because the LEG parameter-space is unconstrained and flexible; for learning, we implemented maximum likelihood inference via BFGS. We found this approach to be simple, scalable, and robust across datasets. The likelihood could also be optimized using Expectation Maximization, but we found it was not as fast [Dempster et al., 1977]. The model could also be fit by moment-matching instead of likelihood; this is a common practice for ARMA models [Brockwell and Davis, 2013] and we hope to explore this possibility in the future.

[1] The requirements of continuity and integrability are too strong. For example, the sinc kernel is not Lebesgue integrable, but it is easy to approximate with a spectral mixture kernel. In the future we hope to refine these conditions.

4.2 Linear computational scaling

As usual in state-space models, problems of evaluation, interpolation, smoothing, and sampling reduce to operations with block-tridiagonal matrices [De Jong, 1988]. This block-tridiagonal structure allows linear-time inference.

4.3 GPU acceleration

Dynamic programming algorithms are the standard tool for analyzing state-space models. Many quantities of interest can be computed using such algorithms [Li, 2009].

To create a dynamic programming algorithm, one must specify one key thing: the variable order. For example, if one uses a simple linear order to the variables, processing them one at a time along the state-space chain, one obtains the popular Kalman Filter algorithm. Unfortunately, this algorithm cannot be easily parallelized to take advantage of modern hardware such as GPUs. If the latent process has a quick mixing time this requirement can be relaxed [Gonzalez et al., 2009], but we seek an algorithm that parallelizes efficiently regardless of the parameters of the model.

The Cyclic Reduction (CR) permutation, well-known in the matrix algorithms literature [Sweet, 1974], provides a natural variable order for creating parallel algorithms with state-space models. Unlike the simple linear-ordering, the CR ordering proceeds in roughly $\log_2 m$ stages, and at each stage the relevant dynamic programming computations can be performed entirely in parallel. The first stage handles every other variable (e.g. all the variables with even-valued indices). The second stage then applies the same idea recursively, processing every other variable of that which remains. For example, given 14 variables, the CR ordering proceeds in 5 stages, given by

$$\overbrace{2,4,6,8,10,12,14}^{1},\overbrace{3,7,11}^{2},\overbrace{5,13}^{3},\overbrace{9}^{4},\overbrace{1}^{5}.$$

Exact details of the algorithms are given in Appendix D, but we here sketch the main ideas.

Recall that everything we need to know about state-space models can be understood in terms of symmetric block-tridiagonal matrix calculations. Eubank and Wang [2002] provide an excellent primer on these connections between state-space models and block-tridiagonal matrices. We found this matrix point of view easier to work with for the purposes of writing code. From this point of view, to compute our state-space analyses we must be able to perform three main operations. Given any block tridiagonal matrix J and any vector x, we need to be able to compute (1) the determinant of J, (2) the value of $J^{-1}x$, and (3) the value of $x^\top J^{-1}x$. Of course, if we can compute $J^{-1}x$ it is trivial to compute $x^\top J^{-1}x$ – but in practice, it turns out that computing $x^\top J^{-1}x$ is much easier; we consider it a separate task.[2]

Dynamic programming algorithms can be used to complete all needed matrix calculations. The `leggps.cr` module performs these computations using dynamic programming with CR ordering; this CR ordering allows us to make efficient use of the GPU. There are four main functions:

- `decompose` – given a block tridiagonal matrix J, use dynamic programming to produce an opaque processed version of J which can be used for further analysis. As discussed in Appendix D, this processed version can be formally understood as the Cholesky decomposition of a version of J in which both rows and columns have been permuted according to the CR ordering.
- `det` – given a decomposition of J computed by `decompose`, compute the determinant of J
- `solve` – given a decomposition of J computed by `decompose`, compute $J^{-1}x$.
- `mahal` – given a vector x and a decomposition of J computed by `decompose`, compute $x^\top J^{-1}x$.

These functions are used by the `leggps` package to compute everything necessary for analyzing state-space models. They also have independent value as the first published pure-python GPU-friendly code for cyclic-reduction-based analyses of symmetric block-tridiagonal matrices.

CR has similarities to other techniques. It is intuitively similar to multigrid techniques [Terzopoulos, 1986, Hackbusch, 2013] which have been used for Gaussian inference in other contexts [Papandreou and Yuille, 2010, Mukadam et al., 2016, Zanella and Roberts, 2017], but CR is a direct exact method whereas multigrid is iterative. CR is quite similar to the associative-scan method developed by Särkkä and García-Fernández [2019]. Like CR, associative scans use parallel

[2] Why is it faster? Essentially because all of these operations involve first computing a decomposition of the form $LL^\top = J$. Thus $x^\top J^{-1}x = \|L^{-1}x\|^2$, which can be computed by solving $Ly = x$. By contrast, computing $J^{-1}x$ is slower because it is achieved in two stages; first one finds z such that $Lz = x$ and then one finds y such that $L^\top y = z$. Thus the computation time for `mahal` is actually roughly half the computation time for `solve`.

hardware to get exact calculations for state-space models. Both CR and the associative-scan methods can be completed with k processors on the order of m/k. In practice, we used CR because we found it easy to write the code to calculate the relevant quantities (e.g. posterior variances). Implementing CR in modern software libraries (TensorFlow2 in this case) was straightforward, making it easy to take advantage of modern hardware.

5 Extensions

Before moving on to illustrate these results with experiments on simulated and real data, we pause to note several useful extensions:

Nonstationary processes. We have focused on stationary processes here for simplicity. A number of potential extensions to nonstationary processes are possible while retaining linear-time scaling. As one example, starting with LEG processes as a base, nonstationary models can be developed using the techniques from Benavoli and Zaffalon [2016].

Non-Gaussian observations. Many approaches have been developed to adapt GP inference methods to non-Gaussian observations, including Laplace approximations, expectation propagation, variational inference, and a variety of specialized Monte Carlo methods [Hartikainen et al., 2011, Riihimäki et al., 2014, Nguyen and Bonilla, 2014, Nishihara et al., 2014]. Many of these can be easily adapted to the LEG model, using the fact that the sum of a block-tridiagonal matrix (from the precision matrix of the LEG prior evaluated at the sampled data points) plus a diagonal matrix (contributed by the likelihood term of each observed data point) is again block-tridiagonal, leading to linear-time updates [Smith and Brown, 2003, Paninski et al., 2010, Fahrmeir and Tutz, 2013, Polson et al., 2013, Khan and Lin, 2017, Nickisch et al., 2018].

Nonlinear domains. Just as Gaussian Markov models in discrete time can be easily extended to Gaussian graphical models on general graphs, it is straightforward to extend the Gaussian Markov PEG and LEG processes to stochastic processes on more general domains with a tree topology, where message-passing can still be applied.

Multidimensional domains. We can also model multidimensional processes of the form $x : \mathbb{R}^d \to \mathbb{R}^n$. Given matrices B, Λ, and collections of matrices N_{rk}, R_{rk}, we construct tensor products of LEG kernels. In particular, consider kernels of the form $\delta_\tau \Lambda\Lambda^\top + \sum_{r=1}^{\zeta} \prod_{k=1}^{d} BC_{\mathrm{PEG}}(\tau_k; N_{rk}, R_{rk})B^\top$. In the supplement we show that such kernels can approximate any continuous integrable kernel. Efficient computation with such kernels is possible if our observations all lie within a (potentially irreguarly-spaced) grid. In the supplement we give an algorithm for efficiently multiplying by the covariance matrix in such a case, and show that the computational cost of this algorithm scales linearly with the number of points in the grid. Combined with efficient preconditioned conjugate gradient methods as implemented in GPyTorch (cf. Gardner et al. [2018]), for example, this approach should yield efficient inference algorithms for such processes.

6 Experiments

We had two questions which we wanted to address empirically.

First, we wanted to know how fast the `leggps` package actually is. Do the cyclic reduction algorithms actually give us better runtimes? How does it compare with the associative scan methods developed in [Särkkä and García-Fernández, 2019]? How does it compare with other Gaussian Process approaches?

Second, we wanted to see if there were any strange pathologies associated with the LEG parameterization. When the rank ℓ is sufficiently high and there is enough data, Theorem 2 suggests LEG models should be able to learn any stationary integrable kernel arbitrarily well. However, it is possible that the LEG parameterization might introduce some unexpected inductive bias into the learning process. We were particularly sensitive to this problem because we had some experience with the Celerité models; these models were designed for astronomical phenomena which feature many regular patterns, and we found these models had a corresponding inductive bias towards periodic covariances. Given samples from models with no cyclic structure, the Celerité models would often yield estimates with large periodic components. To satisfy ourselves that LEG models had no such inductive bias, we looked at a variety of different cases and inspected how well the LEG model family was able to hone in on the truth.

Note that we did not seek to rigorously evaluate whether state-space models are a useful tool for learning, interpolating, and smoothing time series data. This fact is already well-established in the literature, and its discussion is beyond the scope of this paper.

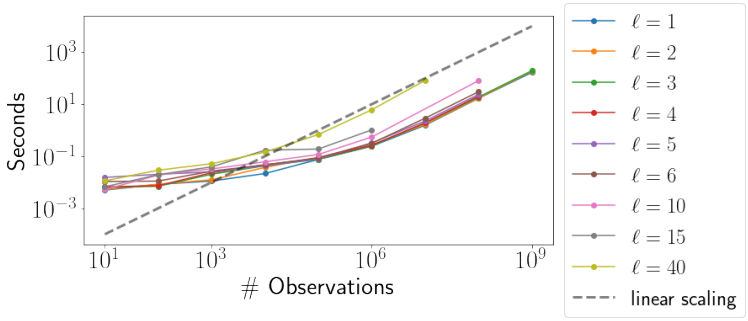

Figure 2: **Walltime for evaluating PEG likelihoods**. How long does it take to compute the likelihood for a PEG model on an m5.24xlarge machine on the Amazon AWS service? We compare times for different ranks (ℓ) and different numbers of blocks (# Observations). For example, the likelihood for one billion observations with $\ell = 3$ can be computed in three and a half minutes. Note that the runtime for these evaluations would not depend on the exact value of the data chosen; for convenience, we evaluated $\mathbb{P}(z = 0)$.

6.1 Is `leggps` fast?

6.1.1 Does CR scale linearly with the number of observations?

In theory, cyclic reduction algorithms should scale linearly with the number of samples. However, we wanted to check if there might be practical difficulties that could get in the way. To do so, we measured how long it took to compute the likelihood for a PEG model. In all cases we evaluated the likelihood $\mathbb{P}(z = 0)$; the runtime is be the same, regardless of where we evaluate the likelihood. We varied both the number of observations and the rank. In each case we used an m5-24xlarge machine on Amazon Web Services (AWS).

Overall, the empirical scaling appeared consistent with the theoretical predictions of linear scaling. The likelihood of one million observations from a rank-3 model could be computed in 0.25 seconds, and one billion observations could be computed in 195 seconds. We saw similar trends across models of other ranks; the results are summarized in Figure 2. Note that for smaller datasets we actually observed a sublinear scaling (i.e. a slope of less than one on the log-log plot) that turns linear for larger values of m.

6.1.2 Can CR take advantage of GPUs?

In theory, the Cyclic Reduction methods used by `leggps` should allow faster computations by making it possible to spread out the work over many cores. However, we wanted to check if there might be practical difficulties that could get in the way. To do so, we compared the `leggps` package with two alternatives: `pylds` (a single-threaded C package for state-space models) and `pyro.distributions.GaussianHMM` (a parallel associative-scan package for state-space models). We also investigated how performance varied between CPU-only hardware and GPU hardware. These experiments yielded three main findings:

- GPU hardware is faster than any number of CPU cores – but with enough samples it becomes impossible to keep everything in GPU memory, so it is not easy to use GPUs to directly compute likelihoods on billions of observations. If the process is expected to mix well within a few million observations, this difficulty can be circumvented by using batches of a few million observations at a time; it may even be possible to learn the parameters using a subset of the data. Once the model is learned on the GPU using this batch-approach, exact smoothing for a much larger dataset can be performed on the CPU. However, if the process has extremely long-range dependencies, new approaches would be necessary. One option would be to break the data into tiles and move the relevant tensors in and out of GPU memory as necessary to compute the relevant quantities. We hope to explore these possibilities in the future.
- CR and associative-scan methods seem to have roughly the same runtimes. Likely as not, any difference in runtime reflects a difference in implementation details (e.g. the `GHMM` package was written in PyTorch, but `leggps` was written in TensorFlow).
- When the number of observations is less than 200, the single-threaded `pylds` package can be slightly faster.

To obtain these results, we used two different measures of speed. To compare CR with associative-scans, we evaluated the time required to compute the gradient of the likelihood of a state-space model with respect to its parameters.

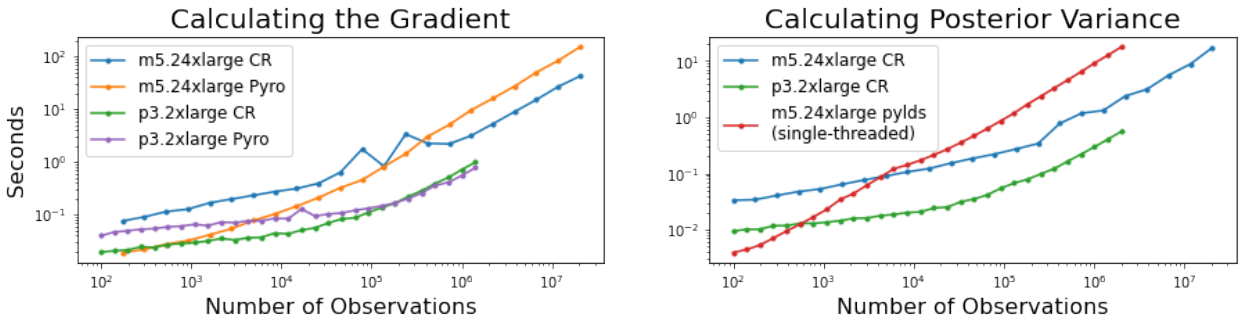

Figure 3: `leggps` **computes with state-of-the-art speed**. Here we evaluate time required to perform two key tasks for inference and learning with state-space models. In each case we assume $\ell = 5, n = 4$; we found similar results for other dimensionalities. We look at three different packages: `pyro.distributions.GaussianHMM` (Pyro), `pylds` (pylds), and `leggps` (CR). We also look at two different types of hardware on Amazon ec2: m5.24xlarge machines (96 cores with 384 gigabytes of RAM) and p3.2xlarge (one Nvidia V100 GPU). These plots suggest three overall findings: Pyro and CR perform comparably, a single GPU is much faster than any number of CPUs, and pylds can be faster when the number of observations is small.

To compare with `pylds`, we evaluated the time required to compute posterior variances. We did not use the same benchmark for both packages because the `pylds` package does not compute gradients and the `GaussianHMM` package does not compute posterior variances.

The times are summarized in Figure 3. Several remarks are in order about these plots:

- When the number of observations is large, the GPU architecture is unable to finish the computations due to RAM limitations.
- We did not run pylds on very large datasets due to the prohibitive time costs.
- We used Amazon hardware to perform our tests. We used m5.24xlarge machines to represent CPU computation (96 cores from Intel Xeon Platinum 8000 processors, 384 gigabytes of memory), and p3.2xlarge machines to represent GPU computation (one Nvidia Tesla V100 processor with 16 gigabytes of memory). Note that the `pylds` package is single-threaded in nature, and unable to take advantage of the 96 cores offered by the m5.24xlarge; this package achieves essentially the same times even with much more modest machines such as the m5.large machine.

6.2 Does `leggps` benchmark well on simulated data?

6.2.1 Can `leggps` estimate classic one-dimensional kernels?

How high does the rank of a LEG model have to be before we can get a good fit to data? We investigate this question by examining several popular one-dimensional kernels. In each case we draw fifty thousand observations, each taken .1 units apart from the next. Figure 4 demonstrates that LEG kernels achieve low error even when the rank ℓ is small.

6.2.2 How does `leggps` compare with other standard tools for estimating GPs?

We benchmarked the LEG approach against two other families of Gaussian Processes: Celerite and Spectral Mixtures. We sampled eighteen thousand observations spaced .1 units apart from GPs with several different kernels: the sum of a Radial Basis Function (RBF) and Rational Quadratic (RQ) kernels, an RBF kernel multiplied by cosine, the sum of an RBF kernel with one-fifth of an RQ kernel, the product of a cosine with the previous kernel, a triangle kernel, and the product of an RBF kernel with a high-frequency cosine. We estimated Celerite parameters using the `celerite2` package and estimated the SM parameters using the `gpytorch` package. All three families include a "rank" hyperparameter (i.e. the rank of LEG models, the number of terms in a Celerite kernel, and the number of mixtures in an SM kernel); in order to give all models the best chance, we exhaustively searched over the possible values of this rank hyperparameter and selected the model with the best likelihood on six thousand held-out samples (the best LEG kernels were of rank 7-11, the best Celerite kernels were of rank 6-7, and the best SM kernels were of rank 4-8). The Spectral Mixture kernels and the LEG kernels appear to perform comparably; the Celerite family is designed for

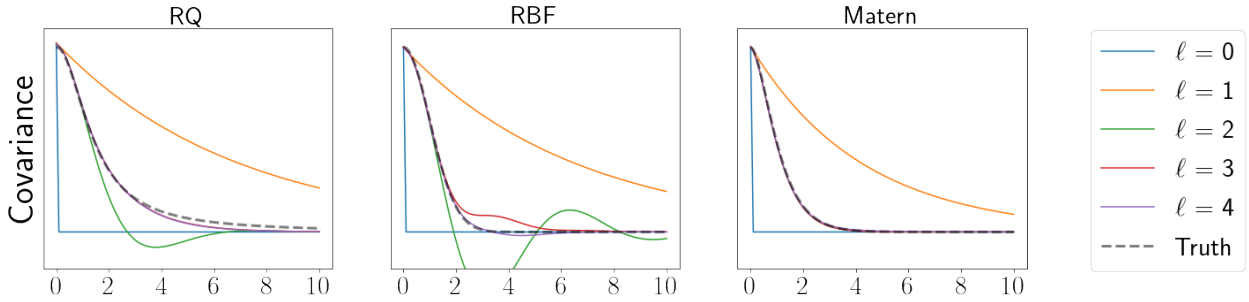

Figure 4: **LEG kernel approximation of some popular specific kernels**. By taking the rank ℓ sufficiently high we can achieve arbitrarily good approximations to any kernel. In the three examples shown here, $\ell = 4$ already provides adequate approximation quality. Note that in some cases some lines aren't visible because they are superimposed on each other; for example, when approximating Matern kernels we find nearly identical models for $\ell \in 2, 3, 4$.

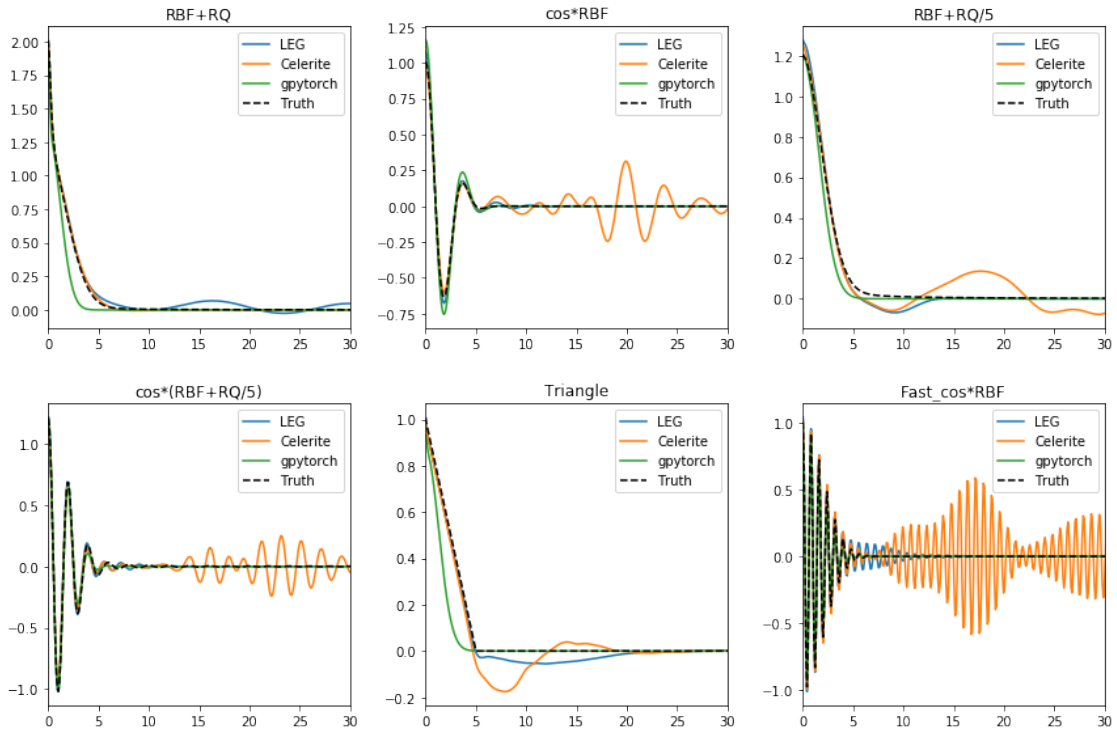

Figure 5: **LEG GPs are fast and accurate**. We tried to learn covariance kernels from data, using maximum likelihood with three different model families: LEG, Celerite, and Spectral Mixtures. We found the LEG and Spectral Mixture kernels to perform comparably; the Celerite estimates performed a bit worse, exhibiting some spurious cyclic activity.

periodic astronomical phenomena, and has a corresponding inductive bias that leads it to estimate overlarge periodic components. These results are summarized in Figure 5.

Note all of these families can achieve any target kernel given sufficiently high rank (as proved in Theorem 2). Thus, these experiments should not be interpreted as evidence regarding the flexibility of these models to learn correct models, given unlimited data. Rather, these experiments show the inductive biases of the three families, given a large dataset with eighteen thousand samples.

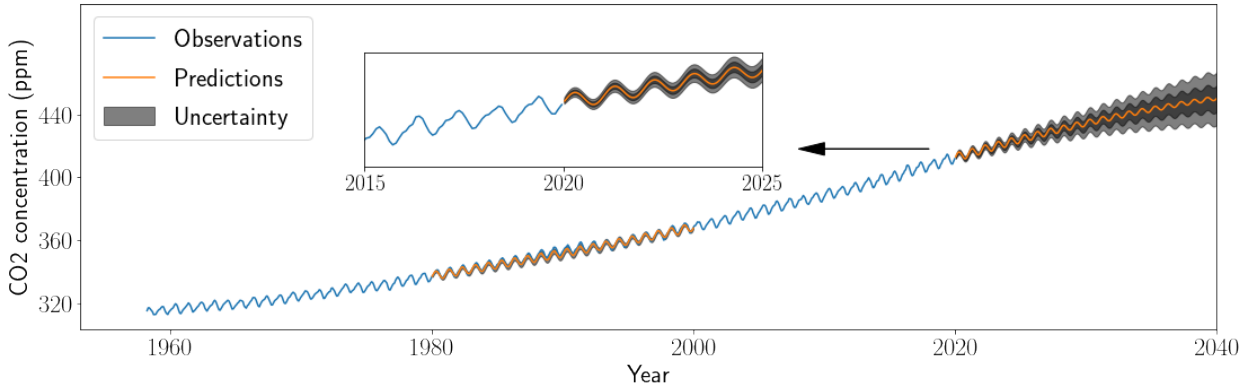

Figure 6: **LEG processes interpolate and extrapolate well across long timescales**. It appears that a rank-5 LEG model is sufficient to capture the linear and periodic trends in the Mauna Loa CO_2 dataset. Above we compare the true observations with interpolations made by the LEG model. The gray areas encompass one and two predictive standard deviations, i.e. the LEG model's uncertainty in forecasting and extrapolating what out-of-sample observations would look like.

6.3 Does `leggps` perform reasonably on real-world data?

6.3.1 Do LEG models perform reasonable interpolation for the Mauna Loa CO_2 dataset?

To check whether LEG parameterization can capture periodic covariances, we turned to the Mauna Loa CO_2 dataset. For the last sixty years, the monthly average atmosphere CO_2 concentrations at the the Mauna Loa Observatory in Hawaii have been recorded [Keeling and Whorf, 2005]. This dataset is interesting because it features two different kinds of structures: an overall upward trend and a yearly cycle. To test the ability of the LEG model to learn these kinds of structures from data, we trained a rank-5 LEG kernel on all the data before 1980 and all the data after 2000. We then asked the LEG model to interpolate what happened in the middle and forecast what the concentration might look like in the next twenty years.

The results are shown in Figure 6. It is encouraging that the LEG predictions interpolate adequately from 1980 to 2000. Even though the LEG process is given no exogenous information about "years" or "seasons," it correctly infers the number of number of bumps between 1980 and 2000. This example shows that the LEG model is sufficiently flexible to learn unanticipated structures in the data.

6.3.2 Do LEG models perform reasonable smoothing for a Hippocampal place-cell dataset?

Finally, we wanted to check whether the LEG approach for covariance estimation might introduce any strange artifacts when applied to irregularly-spaced data.

We looked at observations from neural spiking data [Grosmark and Buzsáki, 2016]. In this data a rat's position in a one-dimensional maze is reported on a regular schedule, around 40 times per second. At each time-step, each neuron may be silent or may fire ("spike") some number of times. For each neuron, we would like to estimate the "tuning curve" – a function which takes in positions and returns the expected number of spikes as a function of the rat's position. With no smoothness assumptions on this function, the problem is impossible; the rat is never observed at exactly the same place twice. However, it is unclear how much smoothness should be assumed. Gaussian Processes offer a natural way to automatically learn an appropriate level of smoothness from the data itself. Note that the observed positions do not fall into a regularly spaced grid, so classical approaches such as the ARMA model cannot be directly applied.

Here we model this tuning curve using a PEG process, $z \sim \mathrm{PEG}(N, R)$. In this view, each data-point from the experiment constitutes a noisy observation of z. When the rat is at position t we model the distribution on the number of spikes observed in a small timebin as a Gaussian, with mean $Bz(t)$ and variance $\Lambda\Lambda^\top$. (It would be interesting to apply a non-Gaussian observation model here, as in, e.g., [Smith and Brown, 2003, Rahnama Rad and Paninski, 2010, Savin and Tkacik, 2016, Gao et al., 2016], and references therein; as noted in section 5, linear-time approximate inference is feasible in this setting and is an important direction for future work.) For each neuron we train the parameters of a separate LEG model. We can then look at the posterior distribution on the underlying tuning curve z. The posterior mean of this process for various neurons is shown in Figure 7. We also represent one standard-deviation of the posterior

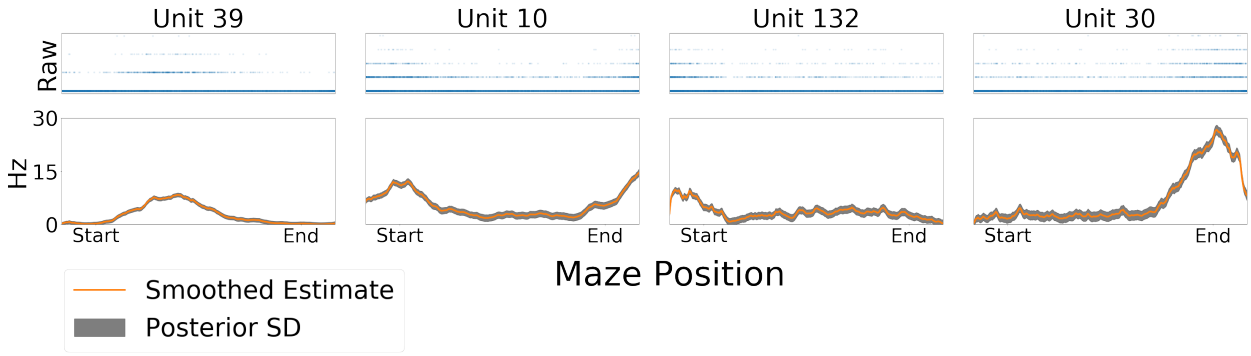

Figure 7: **LEG processes can smooth irregularly spaced neural data**. Ten thousand irregularly spaced observations suggest that the firing rates of hippocampal neurons are modulated by the rat's position in a maze. However, the modulation strength visible in the raw data is weak. By smoothing this data with a LEG process we can see the trend more clearly. How much should we smooth? By training a rank-5 LEG process we can determine a smoothness level automatically. The gray areas indicate the LEG model's posterior uncertainty about the estimated tuning curve.

variance of z with gray shading. Fitting the LEG model and looking at the posterior under the learned model appears to yield an effective Empirical Bayes approach for this kind of data.

7 Conclusions

We here provide several advances for Gaussian Processes on one dimension. First, we show that the LEG model (a particularly tractable continuous-time Gaussian hidden Markov process) can be used to approximate any GP with a stationary integrable continuous kernel, enabling linear runtime scaling in the number of observations. Second, we develop a new unconstrained parameterization of continuous-time state-space models, making it easy to use simple gradient-descent methods. Finally, we develop a simple package for learning, interpolation, and smoothing with such models; this package uses Cyclic Reduction to get rapid runtimes on modern hardware. We believe these advances will open up a wide variety of new applications for GP modeling in highly data-intensive areas involving data sampled at high rates and/or over long intervals, including geophysics, astronomy, high-frequency trading, molecular biology, neuroscience, and more.

Acknowledgements

Thanks to Jake Soloff for resolving a thorny point about matrix-valued measures.

References

Sivaram Ambikasaran, Daniel Foreman-Mackey, Leslie Greengard, David W Hogg, and Michael O'Neil. Fast direct methods for gaussian processes. *IEEE transactions on pattern analysis and machine intelligence*, 38(2):252–265, 2015.

Alessio Benavoli and Marco Zaffalon. State space representation of non-stationary gaussian processes. *arXiv preprint arXiv:1601.01544*, 2016.

R. Bhatia. *Positive Definite Matrices*. Princeton Series in Applied Mathematics. Princeton University Press, 2015. ISBN 9780691168258.

David M Blei, Alp Kucukelbir, and Jon D McAuliffe. Variational inference: A review for statisticians. *Journal of the American statistical Association*, 112(518):859–877, 2017.

P.J. Brockwell and R.A. Davis. *Time Series: Theory and Methods*. Springer Series in Statistics. Springer New York, 2013. ISBN 9781489900043.

Lars Buesing, Jakob H Macke, and Maneesh Sahani. Learning stable, regularised latent models of neural population dynamics. *Network: Computation in Neural Systems*, 23(1-2):24–47, 2012.

Bing Leung Patrick Cheung, Brady Alexander Riedner, Giulio Tononi, and Barry D Van Veen. Estimation of cortical connectivity from eeg using state-space models. *IEEE Transactions on Biomedical engineering*, 57(9):2122–2134, 2010.

Neelam Choudhary, Nicolas Gillis, and Punit Sharma. On approximating the nearest ω-stable matrix. *arXiv preprint arXiv:1901.03069*, 2019.

W. Coffey, Y.P. Kalmykov, and J.T. Waldron. *The Langevin Equation: With Applications to Stochastic Problems in Physics, Chemistry, and Electrical Engineering*. Series in contemporary chemical physics. World Scientific, 2004. ISBN 9789812384621.

John Cunningham, K Shenoy, and Maneesh Sahani. Fast gaussian process methods for point process estimation. In *Proceedings of the International Conference on Machine Learning*, Proceedings of Machine Learning Research, 2008.

Kurt Cutajar, Michael Osborne, Johnn Cunningham, and Maurizio Filippone. Preconditioning kernel matrices. In *Proceedings of the International Conference on Machine Learning*, Proceedings of Machine Learning Research, 2016.

Alexander G De G. Matthews, Mark Van Der Wilk, Tom Nickson, Keisuke Fujii, Alexis Boukouvalas, Pablo León-Villagrá, Zoubin Ghahramani, and James Hensman. Gpflow: A gaussian process library using tensorflow. *The Journal of Machine Learning Research*, 18(1):1299–1304, 2017.

Piet De Jong. The likelihood for a state space model. *Biometrika*, 75(1):165–169, 1988.

Arthur P Dempster, Nan M Laird, and Donald B Rubin. Maximum likelihood from incomplete data via the em algorithm. *Journal of the Royal Statistical Society: Series B (Methodological)*, 39(1):1–22, 1977.

LP Devroye and TJ Wagner. The l1 convergence of kernel density estimates. *The Annals of Statistics*, pages 1136–1139, 1979.

RL Eubank and Suojin Wang. The equivalence between the cholesky decomposition and the kalman filter. *The American Statistician*, 56(1):39–43, 2002.

Ludwig Fahrmeir and Gerhard Tutz. *Multivariate statistical modelling based on generalized linear models*. Springer Science & Business Media, 2013.

Daniel Foreman-Mackey, Eric Agol, Sivaram Ambikasaran, and Ruth Angus. Fast and scalable gaussian process modeling with applications to astronomical time series. *The Astronomical Journal*, 154(6):220, 2017.

Yuanjun Gao, Evan W Archer, Liam Paninski, and John P Cunningham. Linear dynamical neural population models through nonlinear embeddings. In *Advances in neural information processing systems*, pages 163–171, 2016.

Jacob Gardner, Geoff Pleiss, Kilian Q Weinberger, David Bindel, and Andrew G Wilson. Gpytorch: Blackbox matrix-matrix gaussian process inference with gpu acceleration. In *Advances in Neural Information Processing Systems*, pages 7576–7586, 2018.

Elad Gilboa, Yunus Saatçi, and John P Cunningham. Scaling multidimensional inference for structured gaussian processes. *IEEE transactions on pattern analysis and machine intelligence*, 37(2):424–436, 2013.

N Glick. Consistency conditions for probability estimators and integrals of density estimators. *Utilitas Mathematica*, 6: 61–74, 1974.

Joseph Gonzalez, Yucheng Low, and Carlos Guestrin. Residual splash for optimally parallelizing belief propagation. In *Proceedings of Artificial Intelligence and Statistics*, 2009.

Andres D Grosmark and György Buzsáki. Diversity in neural firing dynamics supports both rigid and learned hippocampal sequences. *Science*, 351(6280):1440–1443, 2016.

W. Hackbusch. *Multi-Grid Methods and Applications*. Springer Series in Computational Mathematics. Springer Berlin Heidelberg, 2013. ISBN 9783662024270.

Jouni Hartikainen, Jaakko Riihimäki, and Simo Särkkä. Sparse spatio-temporal gaussian processes with general likelihoods. In *International Conference on Artificial Neural Networks*, pages 193–200. Springer, 2011.

James Hensman, Nicolo Fusi, and Neil D Lawrence. Gaussian processes for big data. In *Uncertainty in Artificial Intelligence*, 2013.

Toni Karvonen and Simo Sarkkä. Approximate state-space gaussian processes via spectral transformation. In *2016 IEEE 26th International Workshop on Machine Learning for Signal Processing*, pages 1–6. IEEE, 2016.

Charles D Keeling and TP Whorf. Atmospheric carbon dioxide record from mauna loa. *Carbon Dioxide Research Group, Scripps Institution of Oceanography, University of California La Jolla, California*, pages 92093–0444, 2005.

Mohammad Emtiyaz Khan and Wu Lin. Conjugate-computation variational inference. In *Proceedings of Artificial Intelligence and Statistics*, 2017.

Stan Z Li. *Markov random field modeling in image analysis*. Springer Science & Business Media, 2009.

Finn Lindgren, Håvard Rue, and Johan Lindström. An explicit link between gaussian fields and gaussian markov random fields: the stochastic partial differential equation approach. *Journal of the Royal Statistical Society: Series B (Statistical Methodology)*, 73(4):423–498, 2011.

Kian Hsiang Low, Jiangbo Yu, Jie Chen, and Patrick Jaillet. Parallel gaussian process regression for big data: Low-rank representation meets markov approximation. In *Twenty-Ninth AAAI Conference on Artificial Intelligence*, 2015.

S. Mergner. *Applications of State Space Models in Finance: An Empirical Analysis of the Time-varying Relationship Between Macroeconomics, Fundamentals and Pan-European Industry Portfolios*. Univ.-Verlag Göttingen, 2009. ISBN 9783941875227.

Mustafa Mukadam, Xinyan Yan, and Byron Boots. Gaussian process motion planning. In *2016 IEEE international conference on robotics and automation*, pages 9–15. IEEE, 2016.

Igor Najfeld and Timothy F Havel. Derivatives of the matrix exponential and their computation. *Advances in applied mathematics*, 16(3):321–375, 1995.

Trung V Nguyen and Edwin V Bonilla. Automated variational inference for gaussian process models. In *Advances in Neural Information Processing Systems*, pages 1404–1412, 2014.

Hannes Nickisch, Arno Solin, and Alexander Grigorevskiy. State space Gaussian processes with non-Gaussian likelihood. In Jennifer Dy and Andreas Krause, editors, *Proceedings of the International Conference on Machine Learning*, volume 80 of *Proceedings of Machine Learning Research*, pages 3789–3798, Stockholmsmässan, Stockholm Sweden, 10–15 Jul 2018. PMLR.

Robert Nishihara, Iain Murray, and Ryan P Adams. Parallel mcmc with generalized elliptical slice sampling. *The Journal of Machine Learning Research*, 15(1):2087–2112, 2014.

Liam Paninski, Yashar Ahmadian, Daniel Gil Ferreira, Shinsuke Koyama, Kamiar Rahnama Rad, Michael Vidne, Joshua Vogelstein, and Wei Wu. A new look at state-space models for neural data. *Journal of computational neuroscience*, 29(1-2):107–126, 2010.

George Papandreou and Alan L Yuille. Gaussian sampling by local perturbations. In *Advances in Neural Information Processing Systems*, pages 1858–1866, 2010.

Nicholas G Polson, James G Scott, and Jesse Windle. Bayesian inference for logistic models using pólya–gamma latent variables. *Journal of the American statistical Association*, 108(504):1339–1349, 2013.

Joaquin Quiñonero-Candela and Carl Edward Rasmussen. A unifying view of sparse approximate gaussian process regression. *Journal of Machine Learning Research*, 6(Dec):1939–1959, 2005.

Kamiar Rahnama Rad and Liam Paninski. Efficient, adaptive estimation of two-dimensional firing rate surfaces via gaussian process methods. *Network: Computation in Neural Systems*, 21(3-4):142–168, 2010.

G.C. Reinsel. *Elements of Multivariate Time Series Analysis*. Springer Series in Statistics. Springer New York, 2003. ISBN 9780387406190.

Jaakko Riihimäki, Aki Vehtari, et al. Laplace approximation for logistic gaussian process density estimation and regression. *Bayesian analysis*, 9(2):425–448, 2014.

S. Särkkä and A. Solin. *Applied Stochastic Differential Equations*. Institute of Mathematical Statistics Textbooks. Cambridge University Press, 2019. ISBN 9781316510087. URL `https://books.google.com/books?id=g5SODwAAQBAJ`.

Simo Särkkä and Ángel F García-Fernández. Temporal parallelization of bayesian filters and smoothers. *arXiv preprint arXiv:1905.13002*, 2019.

Cristina Savin and Gasper Tkacik. Estimating nonlinear neural response functions using gp priors and kronecker methods. In D. D. Lee, M. Sugiyama, U. V. Luxburg, I. Guyon, and R. Garnett, editors, *Advances in Neural Information Processing Systems 29*, pages 3603–3611. 2016.

Anne C Smith and Emery N Brown. Estimating a state-space model from point process observations. *Neural computation*, 15(5):965–991, 2003.

Edward Snelson and Zoubin Ghahramani. Local and global sparse gaussian process approximations. In *Proceedings of Artificial Intelligence and Statistics*, 2007.

Roland A Sweet. A generalized cyclic reduction algorithm. *SIAM Journal on Numerical Analysis*, 11(3):506–520, 1974.

Demetri Terzopoulos. Image analysis using multigrid relaxation methods. *IEEE Transactions on Pattern Analysis and Machine Intelligence*, (2):129–139, 1986.

Theodoros Tsiligkaridis and Alfred O Hero. Covariance estimation in high dimensions via kronecker product expansions. *IEEE Transactions on Signal Processing*, 61(21):5347–5360, 2013.

Aad van der Vaart and Harry van Zanten. Information rates of nonparametric gaussian process methods. *Journal of Machine Learning Research*, 12(Jun):2095–2119, 2011.

P Vatiwutipong and N Phewchean. Alternative way to derive the distribution of the multivariate ornstein–uhlenbeck process. *Advances in Difference Equations*, 2019(1):1–7, 2019.

Ke Wang, Geoff Pleiss, Jacob Gardner, Stephen Tyree, Kilian Q Weinberger, and Andrew Gordon Wilson. Exact gaussian processes on a million data points. In *Advances in Neural Information Processing Systems*, pages 14622–14632, 2019.

Andrew Wilson and Ryan Adams. Gaussian process kernels for pattern discovery and extrapolation. In *Proceedings of the International Conference on Machine Learning*, pages 1067–1075, 2013.

Andrew Wilson and Hannes Nickisch. Kernel interpolation for scalable structured gaussian processes (kiss-gp). In *Proceedings of the International Conference on Machine Learning*, pages 1775–1784, 2015.

Giacomo Zanella and Gareth Roberts. Analysis of the gibbs sampler for gaussian hierarchical models via multigrid decomposition. *arXiv preprint arXiv:1703.06098*, 2017.

Yunong Zhang, William E Leithead, and Douglas J Leith. Time-series gaussian process regression based on toeplitz computation of o (n 2) operations and o (n)-level storage. In *Proceedings of the 44th IEEE Conference on Decision and Control*, pages 3711–3716. IEEE, 2005.

A Supplement Overview

In this supplement we detail the theory and practice for working with Latent Exponentially Generated (LEG) Gaussian Processes.

- Section B is a review about Gaussian Processes of the form $x : \mathbb{R} \to \mathbb{R}^n$ for $n > 1$. This may be helpful for readers which are not familiar with the peculiar matrix-valued spectra of such processes.
- Section C is about the theory of the PEG and LEG models. This section includes proofs for all of the results in the main text. It shows how we arrive at the expression for the covariance of the LEG model. It also details the connection between Spectral Mixture kernels and LEG kernels. This section will be interesting to those seeking to understand why LEG kernels can approximate any Lebesgue-integrable continuous kernel. We conjecture that the conditions of continuity and Lebesgue-integrability are too strong; we hope that an interested reader may be able to figure out how to loosen these conditions.
- Section D is about using Cyclic Reductions to do fast inference with PEG and LEG models. We show how inference with these models is easy as long as we can work efficiently with block-tridiagonal matrices. We define the Cyclic Reduction algorithm for block-tridiagonal matrices and show how it enables us to efficiently compute what we need.
- Section E is about the leggps python package which implements the algorithms from Section 3. This section may be helpful for users of this python code. The leggps package exposes a numpy-based API for learning, finding the posterior, smoothing, interpolating, and forecasting with LEG models (note however that this code uses TensorFlow2 as a backend, so TensorFlow2 must be installed for this code to work). This package also exposes a TensorFlow2-based API for Cyclic Reduction algorithms, which could be used for unrelated applications involving block-tridiagonal matrices.
- Section F includes extensions we would like to implement in the future. For example, we show that LEG kernels can be used to accelerate inference for processes of the form $z : \mathbb{R}^d \to \mathbb{R}^n$; in future we would like to write code to make this vision a reality. If any extensions in this section are important for your work, don't hesitate to raise an issue on the Github Repo at `https://github.com/jacksonloper/leg-gps` and start a conversation.

B Some known facts about GPs

Here we collect some important definitions and facts – already known in the literature – which will be useful in the theory that follows.

B.1 Covariance kernels

Definition 4. Let $z : \mathbb{R} \to \mathbb{R}^\ell$ a Gaussian Process. The covariance kernel of z is given by

$$K(t,s) \triangleq \mathrm{Cov}(z(t), z(s))$$

Note that $K(s,t) = K(t,s)^\top$ (by the definition of a covariance matrix).

Sometimes the covariance kernel only depends on the difference between t and s. Say there exists a matrix-valued function C such that $K(t,s) = C(t-s)$, then K is said to be stationary. In this case, by a slight abuse of terminology, we will call C the covariance kernel of z. Note that $C(-\tau) = C(\tau)^\top$ (again by the definition of a covariance matrix).

For any $C : \mathbb{R} \to \mathbb{R}^{n \times n}$, we will say that C is "nonnegative-definite" if it is the covariance kernel of some Gaussian Process.

B.2 The spectrum of a covariance kernel

Here we consider the spectrum of matrix-valued functions. This spectrum is slightly more involved than the spectra of ordinary functions. To even define it we need to be slightly careful with the complex values involved.

We use the following notation for complex variables in this supplement. Unless it is clear from context that i is being used as an index, we will take $i = \sqrt{-1}$. For any b let $\overline{b}$ denote the **complex conjugate** of b, i.e. if $b = x + iy$ then $\overline{b} = x - iy$. Let the same definition hold elementwise for vectors and matrices, e.g. if $B_{ij} = x + iy$ then $\overline{B}_{ij} = x - iy$. For any matrix B let B^* denote the conjugate transpose, i.e. $B^*_{ij} = \overline{B}_{ji}$. Let $\Re(b) \triangleq (b + \overline{b})/2$ denote the "real part" of b and let $\Im(b) = i(\overline{b} - b)/2$ denote the "imaginary part" of b.

The following Lemma summarizes the results we will need in what follows. These results are already known in the literature.

Proposition 1 (The spectrum of continuous integrable covariance kernels)**.** *Assume $C : \mathbb{R} \to \mathbb{R}^{\ell \times \ell}$ satisfies three properties:*

- *C is continuous.*
- *C is Lebesgue integrable. That is, for each τ let $|C(\tau)| = \sup_x \|C(\tau)x\|/\|x\|$ denote the operator norm of the matrix $C(\tau)$. We require that $\int_0^\infty |C(\tau)| d\tau < \infty$.*
- *C is the covariance kernel of some Gaussian Process $z : \mathbb{R} \to \mathbb{R}^\ell$ (i.e. C is nonnegative-definite).*

We can then find

- *a probability density f on $\mathbb{R}$*
- *a bounded matrix-valued function $M : \mathbb{R} \to \mathbb{C}^{\ell \times \ell}$ such that for almost-every ω we have that $M(\omega)$ Hermitian and nonnegative definite.*

such that

$$C(\tau) = \int e^{-i\tau\omega} f(\omega) M(\omega) d\omega$$

Proof. The continuity of C and the fact that it is a covariance kernel allow us to apply a generalization of Bochner's Theorem to write

$$C(\tau) = \int e^{-i\tau\omega} dF(\omega)$$

for some unique Hermitian-positive-definite-matrix-valued-measure F (cf. [Brockwell and Davis, 2013]).

Now we apply the Lebesgue-integrability condition of C. Since the integral of the operator norm is finite, it follows that the integral of the absolute value of each entry of C is finite – for any $i, j \in \{1 \cdots \ell\}$ we have that $\int |C_{ij}(\tau)| d\tau < \infty$. Now, since C_{ij} (which is integrable) is the Fourier transform of F_{ij}, it follows that F_{ij} has a bounded density with respect to Lebesgue measure. We will denote this as $\tilde{M}_{ij}$, i.e.

$$F(S) = \int_S \tilde{M}(\omega) d\omega$$

Since $F(S)$ is Hermitian and nonnegative definite, it follows that $\tilde{M}(\omega)$ is itself Hermitian and nonnegative definite for almost every ω.

Finally, observe that the measure $S \mapsto \operatorname{tr}(F(S))$ is a finite nonnegative measure. Indeed, $\operatorname{tr} F(\mathbb{R}) = \operatorname{tr} C(0) = \mathbb{E}[\|z(0)\|^2] < \infty$. Thus we may factor $\tilde{M}$ as

$$\tilde{M}(\omega) = M(\omega) f(\omega)$$

where f is a probability density on the real line and M is bounded. □

This leads to the following definitions:

Definition 5. If $\tilde{M}$ is a Hermitian-nonnegative-definite-matrix-valued function such that

$$C(\tau) = \int e^{-i\tau\omega} \tilde{M}(\omega) d\omega$$

then $\tilde{M}$ is called the spectrum of C. If, further, $\tilde{M}(\omega) = M(\omega) f(\omega)$ and f is a probability density, then we will call (M, f) the matrix-scalar factorization of the spectrum of C.

C Theory of PEG and LEG models

We now turn to the definition and theory of the LEG models introduced in the main text. We also study the PEG models upon which the LEG model is built.

C.1 Model definitions

The PEG and LEG models are defined through the following generative story:

1. The PEG model.
   - N, R are $\ell \times \ell$ square matrices.
   - $G = NN^\top + R - R^\top$.
   - $z : \mathbb{R} \to \mathbb{R}^\ell$ is defined by the fact that $Z(0) \sim \mathcal{N}(0, I)$ and

     $$z(t) = z(0) + \int_0^t \left(-\frac{1}{2} G z(s) dt + N dw(s) \right)$$

     for some Brownian motion, w. In this case we say that $z \sim \mathrm{PEG}(N, R)$.
2. The LEG model, formed through an observation model on top of the PEG model:
   - B is an $n \times \ell$ matrix.
   - Λ is an $n \times n$ matrix.
   - For each t independently,

     $$x(t)|z \sim \mathcal{N}(Bz(t), \Lambda\Lambda^T)$$

     where $z \sim \mathrm{PEG}(N, R)$. In this case we say that $x \sim \mathrm{LEG}(N, R, B, \Lambda)$. The dimension of the latent PEG process, ℓ, is called the rank of the LEG process.

C.2 First properties of the PEG and LEG models

The covariance of the PEG model can be written in closed form.

Lemma 1. *$z \sim \mathrm{PEG}(N, R)$ is stationary, with covariance kernel given by*

$$C_{\mathrm{PEG}}(\tau; N, R) \triangleq \exp\left(-\frac{\tau}{2} \left(NN^\top + R - R^\top \right) \right)$$

for $\tau \geq 0$ (for $\tau < 0$ it may readily be computed that $C(\tau)$ must be given by $C(-\tau)^\top$).

Proof. Let $z \sim \mathrm{PEG}(N, R)$, $G = NN^\top + R - R^\top$.

We start by looking at conditional distributions across time. Fix any $t > s$. Per [Vatiwutipong and Phewchean, 2019], we have that

$$\begin{aligned}\mathbb{E}[z(t)|z(s)] &= e^{-G(t-s)/2} z(s) \\ \mathrm{Cov}(z(t)|z(s)) &= e^{-G(t-s)/2} \left(\int_0^{t-s} e^{G\tau/2} N N^\top e^{G^\top \tau/2} d\tau \right) e^{-G^\top (t-s)/2}\end{aligned}$$

To compute this integral, let us consider

$$M(\tau) = \exp(G\tau/2) \exp(G^\top \tau/2)$$

Using the fact that G commutes with $\exp(G)$, we have that

$$\begin{aligned}M'(\tau) &= \frac{1}{2} \exp(G\tau/2)(G + G^\top) \exp(G^\top \tau/2) \\ &= \exp(G\tau/2) N N^T \exp(G^\top \tau/2)\end{aligned}$$

This is precisely the object we were integrating before. The fundamental theorem of calculus therefore gives that

$$\begin{aligned}\mathrm{Cov}(z(t)|z(s)) &= e^{-G(t-s)/2}(M(t-s) - M(0))e^{-G^\top (t-s)/2} \\ &= e^{-G(t-s)/2}(e^{G(t-s)/2} e^{G^\top (t-s)/2} - I)e^{-G^\top (t-s)/2} \\ &= I - e^{-G(t-s)/2} e^{-G^\top (t-s)/2}\end{aligned}$$

Now we will look at unconditional marginal distributions. In particular, fix any any $t > 0$. Using the law of total expectation and the law of total covariance we find that the marginal distribution of $z(t)$ is given by:

$$\begin{aligned}\mathbb{E}[z(t)] &= \mathbb{E}[\mathbb{E}[z(t)|z(0)]] = e^{-G(t-s)/2}\mathbb{E}[z(0)] = 0 \\ \mathrm{Cov}(z(t)) &= \mathbb{E}\left[\mathrm{Cov}(z(t)|z(0))\right] + \mathrm{Cov}(\mathbb{E}[z(t)|z(0)]) \\ &= (I - e^{-G(t-s)/2} e^{-G^\top (t-s)/2}) + (e^{-G(t-s)/2} e^{-G^\top (t-s)/2}) = I\end{aligned}$$

Thus $z(t) \sim \mathcal{N}(0, I)$ for every $t \geq 0$. The same arguments can be applied to show that $z(t) \sim (0, I)$ for $t < 0$.

Finally, we turn to unconditional covariances across time. Since we just showed that the means are all zero it suffices to look at the second-order expectations. Fix $t > s$. We calculate that

$$\begin{aligned}\mathbb{E}[z(t)z(s)^\top] &= \mathbb{E}[\mathbb{E}[z(t)|z(s)]z(s)^\top] \\ &= e^{-G(t-s)/2}\mathbb{E}[\mathbb{E}[z(s)z(s)^\top]] \\ &= e^{-G(t-s)/2}\end{aligned}$$

Note that this depends only upon $t - s$. Together with the fact that the marginals are also the same for every t, this shows that z is stationary. The formula above gives the covariance kernel: $C(\tau) = e^{-G\tau/2}$, as desired. □

A final remark is warranted here about the case $\tau < 0$. In this case, recall that the definition of the covariance matrix gives that $C_{\mathrm{PEG}}(\tau; N, R) = C_{\mathrm{PEG}}(-\tau; N, R)^\top$. Thus a more complete definition of the kernel might be given by

$$C_{\mathrm{PEG}}(\tau; N, R) \triangleq \begin{cases} \exp\left(-\frac{|\tau|}{2}\left(NN^\top + R - R^\top\right)\right) & \tau \geq 0 \\ \exp\left(-\frac{|\tau|}{2}\left(NN^\top + R^\top - R\right)\right) & \tau \leq 0 \end{cases}$$

Now that the covariance of the PEG model is understood, the covariance of the LEG model follows immediately: Let $x \sim \mathrm{LEG}(N, R, B, \Lambda)$. The usual rules for the covariances of Gaussian random variables yield that the covariance of x is given by

$$C_{\mathrm{LEG}}(\tau; N, R, B, \Lambda) \triangleq B\left(C_{\mathrm{PEG}}(\tau; N, R)\right) B^\top + \delta_{\tau=0} \Lambda\Lambda^\top.$$

Here δ is the indicator function.

This representation makes it straightforward to see that the sum of two LEG kernels is itself a LEG kernel. This will be helpful later as we explore connections to Spectral Mixture kernels, which can be understood as a sum of relatively simple kernels.

Proposition 2 (The sum of two LEG kernels is a LEG kernel)**.** *Let* $C(\tau) = C_{\mathrm{LEG}}(\tau; N_1, R_1, B_1, \Lambda_1) + C_{\mathrm{LEG}}(\tau; N_2, R_2, B_2, \Lambda_2)$*. Then there exists* N, R, B, Λ *such that* $C(\tau) = C_{\mathrm{LEG}}(\tau; N, R, B, \Lambda)$ *and the rank of* $C_{\mathrm{LEG}}(\tau; N, R, B, \Lambda)$ *is equal to the the rank of* $C_{\mathrm{LEG}}(\tau; N_1, R_1, B_1, \Lambda_1)$ *plus the rank of* $C_{\mathrm{LEG}}(\tau; N_2, R_2, B_2, \Lambda_2)$*.*

Proof. We can construct it directly:

- N can be constructed as the a direct sum, $N = N_1 \oplus N_2$, i.e.
$$N = \begin{pmatrix} N_1 & 0 \\ 0 & N_2 \end{pmatrix}$$
Note that $\oplus$ is also sometimes used to indicate the Kronecker sum; in this supplement we will always use it to signify the direct sum.
- $R = R_1 \oplus R_2$, i.e.
$$R = \begin{pmatrix} R_1 & 0 \\ 0 & R_2 \end{pmatrix}$$
- $B = (B_1, B_2)$
- Take Λ to be the Cholesky decomposition of $\Lambda_1\Lambda_1^\top + \Lambda_2\Lambda_2^\top$

□

Note that in some cases the sum of two LEG kernels can be written as a LEG kernel whose rank is less than the combined rank of the two constituent LEG kernels. For example, let $C_{\mathrm{LEG}}(N, R, B, \Lambda)$ be a LEG kernel of rank ℓ. Then obviously $C_{\mathrm{LEG}}(N, R, B, \Lambda) + C_{\mathrm{LEG}}(N, R, B, \Lambda)$ can be written as a LEG kernel of rank ℓ.

C.3 Spectrum of the PEG and LEG models

Here we study the spectrum of $C_{\mathrm{PEG}}(\tau; N, R)$. It is is straightforward to write down the spectrum of C in terms of the spectrum of the underlying matrix $G = NN^\top + R - R^\top$. For technical reasons we will here assume that $NN^\top$ is strictly positive definite. When $NN^\top$ is merely nonnegative definite, with some zero eigenvalues, it is no longer possible to represent the spectrum with a matrix-valued function M and things become a bit more complicated. Essentially the same ideas go through, but for simplicity we focus on the positive-definite case here.

Proposition 3. *Let* $NN^\top$ *be strictly positive definite. Then the spectrum of* $C_{\mathrm{PEG}}(N, R)$ *is given by*

$$M_{\mathrm{PEG}}(\omega; N, R) \triangleq \frac{1}{2\pi}\left(\left(\frac{G}{2} - \omega i I\right)^{-1} + \left(\frac{G^\top}{2} + \omega i I\right)^{-1}\right)$$

where $G = NN^\top + R - R^\top$*. That is,*

$$C_{\mathrm{PEG}}(\tau, N, R) = \int_{-\infty}^{\infty} e^{i\omega\tau} M_{\mathrm{PEG}}(\omega; N, R) d\omega$$

for all $\tau \geq 0$*.*

Proof. Since $NN^\top$ is strictly positive definite, the real parts of the eigenvalues of G are also strictly positive, and so $C(\tau)$ decays exponentially as $\tau \to 0$. It follows that $C(\tau)$ is Lebesgue integrable. We can therefore apply the Fourier Inversion formula to argue that the spectrum of C is given by the formula

$$M(\omega) = \frac{1}{2\pi}\int_{-\infty}^{\infty} e^{i\omega\tau} C(\tau) d\tau$$

This integral splits into two parts: positive and negative. Let's look at the positive half first.

$$\begin{aligned}\int_0^{\infty} e^{i\omega\tau} C(\tau) d\tau &= \int_0^{\infty} e^{\tau(i\omega I - G/2)} d\tau \\ &= -(i\omega I - G/2)^{-1} = (G/2 - i\omega I)^{-1}\end{aligned}$$

Here we have used the fact that the derivative of matrix exponentials behaves essentially the same as regular scalar exponentials. Together with the fundamental theorem of calculus, this allows us to get the integral in closed form. Now the negative half:

$$\begin{aligned}\int_{-\infty}^{0} e^{i\omega\tau} C(\tau) d\tau &= \int_{-\infty}^{0} e^{\tau(i\omega I + G^\top/2)} d\tau \\ &= (i\omega I + G^\top/2)^{-1}\end{aligned}$$

Adding the two halves together, we obtain our result. □

Now that we have understood the spectrum of PEG kernels, we turn to the spectrum of LEG kernels. If $\Lambda\Lambda^\top \neq 0$, the LEG kernel is discontinuous and the spectrum becomes technically involved. However, when $\Lambda = 0$ the spectrum will be continuous and is easy to write down:

$$M_{\mathrm{LEG}}(\omega; N, R, B, 0) \triangleq B M_{\mathrm{PEG}}(\omega; N, R) B^T$$

It is straightforward to verify that this is indeed the spectrum i.e.

$$\int e^{-i\tau\omega} M_{\mathrm{LEG}}(\omega; N, R, B, 0) d\omega = C_{\mathrm{LEG}}(\tau; N, R, B, 0)$$

The expression for M_{LEG} suggests that the spectrum of any LEG process decays like an inverse polynomial in ω. This is a relatively slow rate of decay when compared with Radial Basis Function kernels (whose spectrum decays like $\exp(-\omega^2)$) and Rational Quadratic kernels (whose spectrum decays like $\exp(-|\omega|)$). This slow rate of decay in the spectrum allows LEG processes to have "rough" sample paths. This, in turn, permits statistically efficient smoothing even when the underlying function does not have infinitely-many derivatives [Vaart and Zanten, 2011].

C.4 Connections to Celerite and Spectral Mixture kernels

Here we investigate how LEG kernels are related to two model families already known in the literature: Spectral Mixture kernels and Celerite kernels. We'll start by defining these two families of kernels:

C.4.1 Spectral Mixture Kernels

Spectral Mixture (SM) kernels are a family of kernels for Gaussian Processes of the form $z : \mathbb{R}^n \to \mathbb{R}$, introduced in 2013 by Wilson and Adams [Wilson and Adams, 2013]. Here we extend their idea to the kinds of processes we are interested in, namely $z : \mathbb{R} \to \mathbb{R}^n$. For such processes, we define Spectral Mixture (SM) kernels as follows:

Definition 6 (Spectral Mixture Kernels)**.** Let K denote a probability density on $\mathbb{R}$, let $b_1, b_2 \cdots b_\ell \in \mathbb{C}^n$, let $\mu \in \mathbb{R}^\ell$, and let $\gamma > 0$. The **Spectral Mixture kernel with ℓ components** parameterized by p, b, μ, γ is defined by

$$C_{\mathrm{SM}}(\tau; K, b, \mu, \gamma) \triangleq \sum_{k=1}^{\ell} \int e^{-i\omega\tau} b_k b_k^* \gamma K(\gamma(\omega - \mu_k)) d\omega.$$

We will say that a kernel $C_{\mathrm{SM}}(p, b, \mu, \gamma)$ is **based on** K, since it is designed by combining shifted scaled versions of K. Note that C_{SM} is a matrix-valued function, $C_{\mathrm{SM}} : \mathbb{R} \to \mathbb{C}^{n \times n}$.

Note that SM kernels are, in general, complex-valued (we refer the reader back to Section B.2 for the notation we use for such values, e.g. $b^*, \bar{b}, \Re(b), \Im(b)$). For Gaussian Processes we are generally interested in real-valued kernels. In this regards, the following definition and proposition may be helpful:

Definition 7. Let p a probability distribution on $\mathbb{R}$. Let $b \in \mathbb{C}^n$, $\mu \in \mathbb{R}$, and $\gamma > 0$. Let $\tilde{b}_1 = b/2, \tilde{b}_2 = \bar{b}/2, \tilde{\mu}_1 = \mu, \tilde{\mu}_2 = -\mu$. The two-component SM kernel $C_{\mathrm{SM}}(p, \tilde{b}, \tilde{\mu}, \gamma)$ is said to be the **Simple Real** Spectral Mixture kernel arising from p, b, μ, γ.

Proposition 4 (All real SM kernels are sums of Simple Real SM kernels)**.**

1. *Let $C_{\mathrm{SM}}(p, b, \mu, \gamma)$ denote an SM kernel with one component. Let $C_{\mathrm{SM}}(p, \tilde{b}, \tilde{\mu}, \gamma)$ denote the Simple Real SM kernel arising from p, b, μ, γ. Then*

$$C_{\mathrm{SM}}(p, \tilde{b}, \tilde{\mu}, \gamma) = \Re(C_{\mathrm{SM}}(p, b, \mu, \gamma))$$

2. *Let $C_{\mathrm{SM}}(p, b, \mu, \gamma)$ denote any real-valued SM kernel. Then it can be written as the sum of Simple Real SM kernels.*

Proof. The first point follows by observing that that $\Re(x) = (x + \bar{x})/2$.

For the second point. Since $C_{\mathrm{SM}}(p, b, \mu, \gamma)$ is real-valued, it follows that $C_{\mathrm{SM}}(p, b, \mu, \gamma) = \Re(C_{\mathrm{SM}}(p, b, \mu, \gamma))$. Note that $C_{\mathrm{SM}}(p, b, \mu, \gamma)$ is the sum of SM kernels with one component. We can apply the first point to each of these one-component kernels. This yields that $\Re(C_{\mathrm{SM}}(p, b, \mu, \gamma))$ must be the sum of Simple Real SM kernels. □

C.4.2 Celerite kernels

Celerite is a family of kernels for Gaussian Processes of the form $z : \mathbb{R} \to \mathbb{R}$, introduced in 2017 by Foreman-Mackey, Agol, Ambikasaran, and Angu [Foreman-Mackey et al., 2017].

Definition 8. Let $a, b, c, d \in \mathbb{R}^\ell$. The **Celerite kernel with ℓ components** parameterized by a, b, c, d is defined by

$$C_{\mathrm{CEL}}(\tau; a, b, c, d) = \sum_k a_k e^{-c_k \tau} \cos(d_k \tau) + b_k e^{-c_k \tau} \sin(d_k \tau)$$

Note that C_{CEL} is not necessarily positive definite. A **Celerite term** is a Celerite kernel with exactly one component, i.e. $\ell = 1$. As shown in the original paper, a Celerite term $C_{\mathrm{CEL}}(a, b, c, d)$ is positive definite if and only if $|bd| < ac$ and $a, c \geq 0$.

We conjecture that Celerite kernels can also be generalized to Gaussian Processes of the form $z : \mathbb{R} \to \mathbb{R}^n$ for $n > 1$. We leave this for future work.

C.4.3 Connections between the families

How are SM kernels, Celerite kernels, and LEG kernels related?

Lemma 2 (SM kernels, Celerite kernels, LEG kernels)**.**

1. *Every Cauchy-based real-valued SM kernel $C_{\mathrm{SM}} : \mathbb{R} \to \mathbb{R}$ is also a Celerite kernel.*
2. *Every positive-definite Celerite term is also a LEG kernel.*
3. *Every Cauchy-based real-valued SM kernel $C_{\mathrm{SM}} : \mathbb{R} \to \mathbb{R}^{n \times n}$ is also a LEG kernel.*

Proof. We take each point separately.

1. In the original paper [Foreman-Mackey et al., 2017] it is shown that each Simple Real SM kernel based on the Cauchy distribution can be understood as a Celerite term. Proposition 4 thus yields that all Cauchy-based real-valued SM kernels can be understood as Celerite kernels.

2. Let $C_{\mathrm{CEL}}(a, b, c, d)$ denote a positive definite Celerite term. Let

$$\begin{aligned} N_1 &= \sqrt{2c - 2bd/a} \\ R_1 &= \sqrt{2c^2 + 4d^2 + 2b^2 d^2 / a^2} \\ N_2 &= \sqrt{c + bd/a} \end{aligned}$$

   The original Celerite paper shows that positive-definiteness implies $|bd| < ac$ and $a, c \geq 0$, thus $N_1, R_1, N_2 \in \mathbb{R}$. Let

$$N = \begin{pmatrix} N_1 & 0 \\ N_2 & N_2 \end{pmatrix} \qquad R = \begin{pmatrix} 0 & R_1 \\ 0 & 0 \end{pmatrix} \qquad B = \begin{pmatrix} \sqrt{a} & 1 \end{pmatrix}$$

   One can then use a symbolic algebra package (we used sympy) to prove that that the spectrum of $C_{\mathrm{LEG}}(\tau; N, R, B, 0)$ is the same as the spectrum of $C_{\mathrm{CEL}}(\tau; a, b, c, d)$. The formula for the spectrum of the Celerite kernel is given in the original paper and the formula for the spectrum of the LEG kernel follows from Proposition 3.

3. Applying Proposition 2 and 4, we see that it suffices to show that every Simple Real SM kernel based on a Cauchy distribution can be understood as a LEG kernel. Let $C_{\mathrm{SM}}(p, b, \mu, \gamma)$ denote a Simple Real SM kernel. Now define

$$J = \begin{pmatrix} 0 & 1 \\ -1 & 0 \end{pmatrix}$$

and let $\tilde{B} \in \mathbb{R}^{n \times 2}$ be given by $\tilde{B} = \left(\tilde{B}_1, \tilde{B}_2\right)$ such that $b = \tilde{B}_1 + i\tilde{B}_2$. Take $N = I\sqrt{2/\gamma}, R = \mu J$. It is then straighforward to verify that the spectrum of $C_{\mathrm{LEG}}(N, R, \tilde{B}, 0)$ is the same as the spectrum of $C_{\mathrm{SM}}(p, b, \mu, \gamma)$. The formula for the spectrum of the SM kernel is given by definition and the formula for the spectrum of the LEG kernel follows from Proposition 3.

□

This Lemma leads to an open problem. We now know that every positive-definite Celerite term can be understood as a LEG kernel. By Proposition 2 it follows that any sum of positive-definite Celerite terms can be understood as a LEG kernel. However, is it true that every positive-definite Celerite kernel can be understood as a LEG kernel? In general, there exist positive-definite Celerite kernels which are the sum of Celerite terms which are *not all nonnegative-definite*. The negativity of some of the kernels is cancelled out by the positivity in others so that the overall result is positive. Can LEG kernels represent these kinds of Celerite kernels? We leave this question for future work.

C.5 Flexibility of Spectral Mixture Kernels

Just as mixture models can approximate any distribution, it seems reasonable to hope that Spectral Mixture kernels could approximate any stationary kernel. Wilson and Adams already argued this point for SM kernels for processes $z : \mathbb{R}^n \to \mathbb{R}$ [Wilson and Adams, 2013]. Here we show a similar flexibility result for processes of the form $z : \mathbb{R} \to \mathbb{R}^n$.

The key point is the following Theorem, a slight generalization of the usual results for kernel density estimation:

Theorem 1 (Total variation convergence for weighted kernel density estimation)**.** *Let K, p denote bounded densities on $\mathbb{R}^d$. Let $g : \mathbb{R}^d \to [-M, M]$. Let $\gamma_\ell = \ell^{1/2d}$. Let $\mu_1, \mu_2 \cdots \sim p$, independently. For each $\ell \in 1, 2, \cdots$, define $h_\ell(\xi) = \frac{1}{\ell}\sum_{k=1}^{\ell} g(\mu_k)\gamma_\ell^d K(\gamma_\ell(\xi - \mu_k))$. Then*

$$\mathbb{P}\left(\lim_{\ell \to \infty} \int |h_\ell(\xi) - p(\xi)g(\xi)| d\xi = 0\right) = 1.$$

Proof. We largely imitate the proof of Devroye and Wagner [Devroye and Wagner, 1979], which handles the special case that $g(x) = 1$.

For almost any fixed ω, we have that $\lim_{\ell \to \infty} |h_\ell(\omega) - p(\omega)g(\omega)| = 0$ almost surely. This follows from two steps:

1. *Controlling the bias*. Let

$$\begin{aligned} \bar{h}_\ell(\omega) &= \mathbb{E}\left[h_\ell(\omega)\right] \\ &= \int g(x)\gamma_\ell^d K(\gamma_\ell(\omega - x))p(x)dx \end{aligned}$$

Now fix any $\delta > 0$. We have that

$$\begin{aligned} |\bar{h}_\ell(\omega) - p(\omega)g(\omega)| \leq &\int_{\|x-\omega\| < \delta/\gamma_\ell} |p(x)g(x) - p(\omega)g(\omega)|\gamma_\ell^d K(\gamma_\ell(\omega - x))dx \\ &+ \int_{\|x-\omega\| \geq \delta/\gamma_\ell} |p(x)g(x) - p(\omega)g(\omega)|\gamma_\ell^d K(\gamma_\ell(\omega - x))dx \end{aligned}$$

We look at each term separately:

- For $x \approx \omega$ we apply the Lebesgue differentiation theorem. Let $c = \sup K(x)$ and let $\lambda(\delta)$ denote the volume of the ball of radius δ. Noting that $\gamma_\ell^d = \lambda(\delta)/\lambda(\delta/\gamma_\ell)$, we see that the integral of the error over $\|x - \omega\| < \delta/\gamma_\ell$ is bounded by

$$c\lambda(\delta)\frac{1}{\lambda(\delta/\gamma_\ell)}\int_{\|x-\omega\|<\delta/\gamma_\ell} |p(x)g(x) - p(\omega)g(\omega)|dx$$

  For any fixed δ, the Lebesgue differentiation theorem shows that this goes to zero almost everywhere because $\gamma \to \infty$.
- For $\|x - \omega\| > \delta/\gamma_\ell$. Let $c = M \sup_x p(x)$. Then the integral of the error over this domain is bounded by

$$2c\int_{\|x-\omega\|\geq\delta} K(\omega - x)dx$$

  Note that we used a change of variables to drop any dependency on γ_ℓ. Since K is a density we can always find δ so that this is arbitrarily small.

Therefore, for any fixed ε we can always find a δ which ensures that the second term is less than $\varepsilon/2$, and then ensure that the first term is less than $\varepsilon/2$ for all sufficiently large ℓ. In short, $|\bar{h}_\ell(\omega) - p(\omega)g(\omega))| \to 0$ for each ω.

2. *Controlling the variation*. Now we would like to bound $\bar{h}_\ell(\omega) - h_\ell(\omega)$. To do this we note that it is a sum of independent random variables of the form $g(\mu_k)\gamma_\ell^d K(\gamma_\ell(\omega - \mu_k))/\ell$. Letting $c = M \sup_x K(x)$ we observe that the absolute value of each random variable is bounded by $\gamma^d c/\ell$. Hoeffding's inequality then gives that

$$\mathbb{P}\left(\left|\bar{h}_\ell(\omega) - h_\ell(\omega)\right| > \varepsilon\right) \leq 2\exp\left(-\frac{2\ell t^2}{\gamma_\ell^d c}\right) = 2\exp\left(-\sqrt{\ell}\frac{2t^2}{c}\right)$$

   The right-hand-side is always summable for any $t > 0$. Indeed, one may readily verify that if $f(x) = -2\exp(-c\sqrt{x})(c\sqrt{x}+1)/c^2$, then $f'(x) = \exp(-c\sqrt{x})$. For any $c > 0$ it follows that $\int_1^\infty \exp\left(-c\sqrt{x}\right) dx = 2(c+1)e^{-c}/c^2 < \infty$ and

$$\sum_\ell \mathbb{P}\left(\left|\bar{h}_\ell(\omega) - h_\ell(\omega)\right| > \varepsilon\right) < \infty$$

   Applying Borel-Cantelli we find that $|\bar{h}_{y,\ell}(\omega) - h_{y,\ell}(\omega)|$ converges almost surely to zero.

Combining these steps together, we obtain a pointwise result: for almost every ω, the sequence $h_1(\omega), h_2(\omega), \cdots$ converges almost surely to $p(\omega)g(\omega)$.

To complete the proof we must extend this pointwise result to $\mathscr{L}^1$. To do so we start by noting that $\int |h_\ell(\omega)|d\omega \to \int |p(\omega)g(\omega)|d\omega$ almost surely. Indeed, we have that

$$\int |h_\ell(\omega)|d\omega = \frac{1}{\ell}\sum_{k=1}^{\ell} |g(\mu_k)|$$

Since g is bounded, the law of large numbers gives us that this converges almost surely to $|p(\omega)g(\omega)|d\omega$. This allows us to extend our pointwise result to the desired $\mathscr{L}^1$ result via Lemma 3, below. □

For the benefit of the reader we here include a statement of Glick's extension to Scheffe's lemma, as used in the proof above:

Lemma 3 (Glick's extension of Scheffe's lemma)**.** *Let $(\Omega, \mathcal{F}, \pi)$ a probability measure space. Let $h_1, h_2, h_3 \cdots$ denote a sequence of $\mathcal{F}$-measurable functions of the form $h_\ell : \mathbb{R}^d \times \Omega \to \mathbb{R}$. Let $h_\infty : \mathbb{R}^d \to \mathbb{R}$ another function. For π-almost-every x and π-almost-every ω, assume that $\lim_{\ell\to\infty} h_\ell(x,\omega), h_2(x,\omega) = h_\infty(x)$. For π-almost-every ω, assume that $\lim_{\ell\to\infty} \int |h_1(x,\omega)|dx = \int |h_\infty(x,\omega)|dx$, π-almost-surely. Then, for π-almost-every ω, we have that*

$$\lim_{\ell\to\infty} \int |h_\ell(x,\omega) - h_\infty(x)|dx = 0$$

Proof. Apply Scheffe's lemma for each ω. This observation is generally credited to Glick [Glick, 1974]. □

Theorem 1 makes it straightforward to show that SM kernels (and, by extension LEG kernels) can be used to approximate any integrable continuous kernel:

Corollary 1 (Flexibility of Spectral Mixture kernels)**.** *Fix K, a bounded probability density on $\mathbb{R}^n$, $\varepsilon > 0$, and any Lebesgue-integrable continuous positive definite*[3] *stationary kernel $\Sigma : \mathbb{R} \to \mathbb{C}^{n\times n}$. There exists a real valued kernel $C = C_{\mathrm{SM}}(K, b, \mu, \gamma)$ such that the spectral norm of $C(\tau) - \Sigma(\tau)$ is at most ε for every $\tau \in \mathbb{R}$.*

Proof. Apply Proposition 1 to obtain the matrix-scalar factorization of the spectrum of Σ, i.e.

$$\Sigma(\tau) = \int e^{i\tau\omega} f(\omega) M(\omega) d\omega$$

where M is bounded, $M(\tau)$ is Hermitian nonnegative definite for each τ, and f is a probability density. Apply a unitary eigendecomposition to each M, i.e. write

$$\Sigma(\tau) = \sum_{k=1}^{n} \int e^{i\tau\omega} b_k(\omega) b_k^*(\omega) f(\omega) d\omega$$

Now draw $\mu_1, \mu_2 \cdots$ i.i.d from f. For any i, j we may apply Theorem 1 with $g(\omega) = \sum_k b_{ki}(\omega)\overline{b_{kj}}(\omega)$. Indeed, let us adopt the notation

$$\mu^{(\ell)} = \overbrace{\mu_1, \mu_1, \mu_1 \cdots \mu_1}^{n \text{ copies}}, \overbrace{\mu_2, \cdots \mu_2}^{n \text{ copies}}, \cdots \overbrace{\mu_\ell, \cdots \mu_\ell}^{n \text{ copies}}$$

and

$$b^{(\ell)} = b_1(\mu_1), b_2(\mu_1) \cdots b_n(\mu_1), b_1(\mu_2), b_2(\mu_2) \cdots b_n(\mu_2), \cdots b_1(\mu_\ell), b_2(\mu_\ell) \cdots b_n(\mu_\ell)$$

Then Theorem 1 gives that

$$\int |((M(\omega))_{ij} - (M_{\mathrm{SM}}(\omega; K, b^{(\ell)}, \mu^{(\ell)}, \sqrt{n\ell})))_{ij}| d\omega$$

vanishes almost surely for each $i, j \in 1 \cdots n$ as $\ell \to \infty$. Since n is finite it follows that this this result holds for *every* entry i, j. It then follows directly that

$$\sup_z \frac{1}{\|z\|} \int \|M(\omega)z - M_{\mathrm{SM}}(\omega)z\| d\omega$$

also vanishes almost-surely.

So far, we have showed that we can asymptotically match the spectrum of any Lebesgue-integrable continuous positive definite stationary kernel with the spectrum of an SM kernel (at least in an integrated sense, integrated over all frequencies ω). Now we will use this fact to show that we can match the kernel itself. We have that

$$\begin{aligned}\sup_{z,\tau} \frac{1}{\|z\|} \|\Sigma(\tau)z - C_{\mathrm{SM}}(\tau)z\| &\le \sup_{z,\tau} \frac{1}{\|z\|} \int \|e^{i\tau\omega} \times (M(\omega)z - M_{\mathrm{SM}}(\omega)z)\| d\omega \\ &\le \sup_z \frac{1}{\|z\|} \int 1 \times \|M(\omega)z - M_{\mathrm{SM}}(\omega)z\| d\omega\end{aligned}$$

As we showed above, this last quantity vanishes asymptotically as $\ell \to \infty$.

There is one final point that must be made. The statement of this theorem requires that C is real-valued, but the kernels described above may not be perfectly real-valued. To complete our proof, note that if the kernel is arbitrarily close to the correct kernel it will be arbitrarily close to real already; summing the resulting kernel with its complex conjugate yields another SM kernel which is still close to the target and also real-valued. □

Theorem 2 (Flexibility of LEG and Celerite kernels)**.** *For every $\varepsilon > 0$ and every Lebesgue-integrable continuous positive definite stationary kernel $\Sigma : \mathbb{R} \to \mathbb{R}^{n\times n}$ there exists a Celerite kernel C such that the spectral norm of $C(\tau) - \Sigma(\tau)$ is at most ε for every $\tau > 0$. Moreover, there exists a LEG kernel with the same guarantee.*

Proof. Combine Corollary 1 and Lemma 2. □

[3] The requirements of continuity and integrability are too strong. For example, the sinc kernel is not Lebesgue integrable, but it is easy to approximate with a spectral mixture kernel. In the future we hope to refine these conditions.

D Algorithms for LEG processes

D.1 The importance of block-tridiagonal matrices

There are a number of tasks related to the LEG model which we would like to be able to solve efficiently. It turns out that the computationally intensive part of all of these tasks involves working with block-tridiagonal matrices. Here we will look at some common tasks and see how this plays out.

Throughout what follows, we will assume

- $z \sim \mathrm{PEG}(N, R)$
- $t_1 \leq t_2 \leq \cdots \leq t_m$
- $\vec{x}_i \sim \mathcal{N}\left(Bz(t_i), \Lambda\Lambda^T\right)$, independently for each i
- $\vec{z} = (z(t_1) \cdots z(t_n))$

There is a slight subtlety that occurs when $t_i = t_{i+1}$ for some i. However, when this happens we can effectively reduce the problem to a case where the times are distinct by "combining" multiple observations into one. To keep the exposition clear, we will here assume that $t_1 < t_2 < t_3 \cdots t_m$, though the the leggps package can cope with the more general case.

We may be interested in...

- Computing the covariance of $\vec{z}$ and the inverse of that covariance. As shown by Lemma 1, the covariance of $\vec{z}$ can be expressed in terms of $\ell \times \ell$ blocks as follows:

$$\Sigma = \begin{pmatrix} I & e^{-\frac{1}{2}|t_1-t_2|G^T} & e^{-\frac{1}{2}|t_1-t_3|G^T} & \cdots \\ e^{-\frac{1}{2}|t_1-t_2|G} & I & e^{-\frac{1}{2}|t_1-t_2|G^T} & \\ e^{-\frac{1}{2}|t_1-t_3|G} & e^{-\frac{1}{2}|t_1-t_2|G^T} & I & \\ \vdots & & & \ddots \end{pmatrix}$$

  One can readily verify that the the inverse is given by the block-tridiagonal matrix

$$\Sigma^{-1} = \begin{pmatrix} R_1 & O_1^T & 0 & \cdots \\ O_1 & R_2 & O_1^T & \\ 0 & O_2 & R_3 & \\ \vdots & & & \ddots \end{pmatrix}$$

  where

$$d_i = \begin{cases} \infty & i = 0 \\ t_{i+1} - t_i & i \in \{1 \cdots m\} \\ \infty & i = m+1 \end{cases}$$

$$R_i = -(I - e^{-\frac{1}{2}d_i G^T} e^{-\frac{1}{2}d_i G})^{-1} e^{-\frac{1}{2}d_i G^T}$$

$$O_i = I + e^{-\frac{1}{2}d_{i-1}G}(I - e^{-\frac{1}{2}d_{i-1}G^T} e^{-\frac{1}{2}d_{i-1}G})^{-1} e^{-\frac{1}{2}d_{i-1}G^T} + e^{-\frac{1}{2}d_i G^T}(I - e^{-\frac{1}{2}d_i G} e^{-\frac{1}{2}d_i G^T})^{-1} e^{-\frac{1}{2}d_i G}$$

- Computing the likelihood, $\log p(\vec{x})$. Let

$$\tilde{B} = \bigoplus_{i=1}^{m} B$$

$$\tilde{\Lambda} = \bigoplus_{i=1}^{m} \left(\Lambda\Lambda^T\right)$$

  Here by $\oplus$ we signify the direct sum (not the Kronecker sum). For example, $\tilde{B}$ is a block-diagonal matrix with m diagonal blocks, each of which is identically equal to B:

$$\tilde{B} = \begin{pmatrix} B & 0 & 0 & \cdots \\ 0 & B & 0 & \cdots \\ 0 & 0 & B & \cdots \\ \vdots & \vdots & \vdots & \ddots \end{pmatrix}$$

Note that $\tilde{B}$ is not necessarily a square matrix, since B is not necessarily a square matrix. $\tilde{\Lambda} = \oplus(\Lambda\Lambda^\top)$ is constructed similarly, and it is always a square matrix because $\Lambda\Lambda^\top$ is a square matrix.

In terms of these objects, the covariance of $\vec{x}$ is given by

$$\mathrm{Cov}(\vec{x}) = \tilde{B}\Sigma\tilde{B}^T + \tilde{\Lambda}$$

And so the likelihood is given by

$$\begin{aligned}\log p(x) = &-\frac{1}{2}x^T\left(\tilde{B}\Sigma\tilde{B}^T + \tilde{\Lambda}\right)^{-1}x \\ &- \frac{1}{2}\log\left|2\pi\left(\tilde{B}\Sigma\tilde{B}^T + \tilde{\Lambda}\right)\right|\end{aligned}$$

where $|\cdot|$ here denotes the determinant. Let's take one term at a time:

- The Mahalanobis term. The Sherman-Morrison formula gives that

$$\begin{aligned}x^T\left(\tilde{B}\Sigma\tilde{B}^T + \tilde{\Lambda}\right)^{-1}x &= x^T\left(\tilde{\Lambda}^{-1} - \tilde{\Lambda}^{-1}B^T\left(\Sigma^{-1} + B^T\tilde{\Lambda}^{-1}B\right)^{-1}B^T\tilde{\Lambda}^{-1}\right)x \\ &= x^T\tilde{\Lambda}^{-1}x - x^T\tilde{\Lambda}^{-1}B^T\left(\Sigma^{-1} + B^T\tilde{\Lambda}^{-1}B\right)^{-1}B^T\tilde{\Lambda}^{-1}x\end{aligned}$$

  The hard part in computing this is solving the linear system

$$\left(\Sigma^{-1} + B^T\tilde{\Lambda}^{-1}B\right)^{-1}\left(B^T\tilde{\Lambda}^{-1}x\right) = ?$$

  Fortunately, the matrix $\Sigma^{-1} + B^T\tilde{\Lambda}^{-1}B$ is block-tridiagonal. So if we can compute solves with block-tridiagonal matrices this is not a problem.
- The determinant term. The Matrix Determinant Lemma gives that

$$\left|\tilde{B}\Sigma\tilde{B}^T + \tilde{\Lambda}\right| = \frac{\left|\tilde{\Lambda}\right|}{\left|\Sigma^{-1}\right|}\left|\Sigma^{-1} + B^T\tilde{\Lambda}^{-1}B\right|$$

  The hard part here is computing the determinant of $\left|\Sigma^{-1}\right|$ and $\left|\Sigma^{-1} + B^T\tilde{\Lambda}^{-1}B\right|$. Again, these are block-tridiagonal matrices. So if we can do that we have no problem.

- In-sample posterior estimates. Here we are interested in computing $\mathbb{E}\left[\vec{z}|\vec{x}\right], \mathrm{Cov}\left(\vec{z}|\vec{x}\right)$. We calculate that

$$\begin{aligned}\mathbb{E}\left[\vec{z}|\vec{x}\right] &= \left(\Sigma^{-1} + B^T\tilde{\Lambda}^{-1}B\right)^{-1}\left(B^T\tilde{\Lambda}^{-1}x\right) \\ \mathrm{Cov}\left(\vec{z}|\vec{x}\right) &= \left(\Sigma^{-1} + B^T\tilde{\Lambda}^{-1}B\right)^{-1}\end{aligned}$$

  Thus to compute the first object we need to be able to compute solves with block-tridiagonal matrices. To compute the second object we need to be able to invert block-tridiagonal matrices. As we shall see, computing every entry in this inverse is intractable, but computing the diagonal and off-diagonal blocks can be done efficiently. This is sufficient to find the marginal in-sample posterior distributions for each $\vec{z}_k$.

- Out-of-sample posterior estimates. Here we are interested in computing $\mathbb{E}\left[\vec{z}(t)|\vec{x}\right], \mathrm{Cov}\left(\vec{z}(t)|\vec{x}\right)$ for arbitrary t. There are four different cases here:
  - If $t = t_i$ for some i, then we should use the in-sample posterior estimates.
  - If $t > t_m$, then we have a forecasting problem. The Markov structure gives that

$$p(z(t)|\vec{x}) = \int p(z(t)|\vec{z}_m)p(\vec{z}_m|\vec{x})d\vec{z}_m$$

    The distribution of $p(z(t)|z(t_m))$ is found in closed-form by using the covariance formulas for the PEG process. Thus we can compute the marginal distribution of $z(t)|\vec{x}$ as long as we know the marginal distribution of $\vec{z}_m|\vec{x}$. This requires knowing the in-sample posterior mean and final diagonal block of the in-sample posterior covariance.

  - If $t_i < t < t_{i+1}$ we have an interpolation problem. In this case the Markov structure gives that

$$p(z(t)|\vec{x}) = \iint p(z(t)|\vec{z}_i, \vec{z}_{i+1}) p(\vec{z}_i, \vec{z}_{i+1}|\vec{x}) d\vec{z}_i d\vec{z}_{i+1}$$

    The distribution of $p(z(t)|\vec{z}_i, \vec{z}_{i+1})$ is found in closed-form by using the covariance formulas for the PEG process. Thus we can compute the marginal distribution of $z(t)|\vec{x}$ as long as we know the marginal distribution of $\vec{z}_i, \vec{z}_{i+1}|\vec{x}$. This requires knowing the in-sample posterior mean and the diagonal and off-diagonal blocks of the in-sample posterior covariance.
  - If $t < t_1$, we have a backwards forecasting problem. This is essentially the same as the forward forecasting problem, but the PEG process covariance formulas are slightly different.

- Smoothing/forecasting. Here we are interested in a few related things, all of which follow immediately from the out-of-sample posterior estimates.
  - The posterior predictive means:

$$\mathbb{E}\left[B\vec{z}(t)|\vec{x}\right] = B\mathbb{E}\left[\vec{z}(t)|\vec{x}\right]$$

  - The posterior predictive uncertainty:

$$B^T \text{Cov}\left[z(t)|\vec{x}\right] B^T$$

    This represents the uncertainty we have about the posterior predictive means.
  - The posterior predictive variances:

$$B^T \text{Cov}\left[z(t)|\vec{x}\right] B^T + \Lambda\Lambda^T$$

    This is the conditional variance of a new sample taken at position t.

In conclusion, we see that all of the things we need to do can be achieved efficiently as long as we can...

- Solve $J^{-1}x$ when J is block-tridiagonal.
- Compute the determinant $|J|$ when J is block-tridiagonal.
- Compute the diagonal and off-diagonal blocks of the inverse of J^{-1} when J is block-tridiagonal.

D.2 Computations with block-tridiagonal matrices using Cyclic Reduction (CR)

Above we saw that most common tasks with LEG processes amount to computations with block-tridiagonal matrices. Cyclic Reduction (CR) is a classic technique for efficient parallel computations with such matrices [Sweet, 1974]. These techniques appear to be relatively unknown in the Machine Learning literature, and the original text is a bit dense. We here describe the algorithms involved in CR.

Let J be the symmetric positive-definite block-tridiagonal matrix, defined blockwise by

$$J = \begin{pmatrix} R_0 & O_0^T & 0 & \cdots \\ O_0 & R_1 & O_1^T & \\ 0 & O_1 & R_2 & \\ \vdots & & & \ddots \end{pmatrix}$$

We would like to be able to compute efficiently with J. To do so, we start by decomposing J using what is called a "Cyclic Reduction." This gives us a convenient representation of J which is easy to work with. Here's how it works.

Definition 9 (Cyclic Reduction)**.** For each m, let P_m

$$P_m = \begin{pmatrix} I & 0 & 0 & 0 & 0 & \\ 0 & 0 & I & 0 & 0 & \\ 0 & 0 & 0 & 0 & I & \\ & & & & & \ddots \end{pmatrix}$$

denote the permutation matrix which selects every other block of a matrix with m blocks. Let

$$Q_m = \begin{pmatrix} 0 & I & 0 & 0 & 0 & \\ 0 & 0 & 0 & I & 0 & \\ 0 & 0 & 0 & 0 & 0 & \\ & & & & & \ddots \end{pmatrix}$$

denote the complementary matrix, which takes the other half of the blocks.

The **Cyclic Reduction** of a block-tridiagonal matrix J with m blocks is defined recursively by

$$\begin{aligned} L = \text{CyclicReduction}\,(J, m) = \begin{pmatrix} P_m^T & Q_m^T \end{pmatrix} \begin{pmatrix} D & 0 \\ U & \tilde{L} \end{pmatrix} \\ D = \text{Cholesky}\left(P_m J P_m^\top\right) \\ U = Q_m J P_m^T D^{-\top} \\ \tilde{J} = Q_m J Q_m^T - U^\top U \\ \tilde{L} = \text{CyclicReduction}\left(\tilde{J}, \lceil m/2 \rceil\right) \end{aligned}$$

What are these P, Q matrices doing? They are simply selecting subsets of blocks of the matrices involved. For example, it is straightforward to show that $P_m J P_m^\top$ is block-diagonal, with blocks given by $R_0, R_2, R_4, \cdots$. The matrix $Q_m J Q_m^\top$ is also block-tridiagonal, with blocks given by $R_1, R_3, R_5, \cdots$. The matrix $Q_m J P_m^\top$ is upper block-didiagonal (i.e. it has diagonal blocks and one set of upper off-diagonal blocks); the diagonal blocks are given by $O_0, O_2, O_4, \cdots$ and the upper off-diagonal blocks are given by $O_1, O_3, O_5, \cdots$.

For this recursive algorithm to make sense, we need that $\tilde{J}$ is also block-tridiagonal – but this is always true if J is block-tridiagonal. The recursion terminates when J has exactly one block. For this we define the base-case

$$\text{CyclicReduction}\,(J, 1) = \text{Cholesky}(J)$$

Proposition 5. *Let* $L = \text{CyclicReduction}\,(J, n)$. *Then* $LL^\top = J$.

Proof. By induction. For the case $n = 1$ the algorithm works because the Cholesky decomposition works.

Now let us assume the algorithm works for all $\tilde{n} < n$. We will show it works for m. Let

$$\begin{aligned} L = \begin{pmatrix} P_m^T & Q_m^T \end{pmatrix} \begin{pmatrix} D & 0 \\ U & \tilde{L} \end{pmatrix} \\ D = \text{Cholesky}\left(P_m J P_m^\top\right) \\ U = Q_m J P_m^T D^{-\top} \\ \tilde{J} = Q_m J Q_m^T - U^\top U \\ \tilde{L} = \text{CyclicReduction}\left(\tilde{J}, \lceil m/2 \rceil\right) \end{aligned}$$

By induction $\tilde{L}\tilde{L}^\top = \tilde{J}$. Thus

$$\begin{aligned} LL^T &= \begin{pmatrix} P_m^T & Q_m^T \end{pmatrix} \begin{pmatrix} D & 0 \\ U & \tilde{L} \end{pmatrix} \begin{pmatrix} D^T & U^T \\ 0 & \tilde{L}^T \end{pmatrix} \begin{pmatrix} P_m \\ Q_m \end{pmatrix} \\ &= \begin{pmatrix} P_m^T & Q_m^T \end{pmatrix} \begin{pmatrix} DD^T & DU^T \\ UD^T & UU^T + \tilde{L}\tilde{L}^T \end{pmatrix} \begin{pmatrix} P_m \\ Q_m \end{pmatrix} \\ &= \begin{pmatrix} P_m^T & Q_m^T \end{pmatrix} \begin{pmatrix} P_m J P_m^T & \cancel{DD^{-1}} P_m J Q_m^T \\ Q_m J P_m^T \cancel{D^{-T} D^T} & \cancel{UU^T} + Q_m J Q_m^T - \cancel{UU^T} \end{pmatrix} \begin{pmatrix} P_m \\ Q_m \end{pmatrix} \\ &= J \end{aligned}$$

□

This decomposition enables efficient computations with J. Below we describe all of the relevant algorithms (including the CR decomposition algorithm itself) from an algorithms point of view, giving runtimes as we go. We will see that all operation counts scale linearly in the number of blocks. We will also discuss parallelization; as we shall see, almost all of the work of a Cyclic Reduction iteration can be done in parallel across the m blocks of J.

D.2.1 CyclicReduction

Algorithm 1: decompose

input : rblocks,oblocks,m – the diagonal and lower off-diagonal blocks of a block-tridiagonal matrix J which has m blocks

output : dlist,flist,glist– a representation of the CR decomposition of J

1 **if** $m = 1$ **then**

2 **return** $[\text{Cholesky}(R_0)], [], []$

3 **else**

4 Adopt the notation R_i =rblocks[i] and O_i =oblocks[i];

5 Let

$$D \triangleq \begin{pmatrix} D_0 & 0 & 0 \\ 0 & D_1 & \\ & & \ddots \end{pmatrix} \triangleq \begin{pmatrix} \text{Cholesky}\,(R_0) & 0 & 0 \\ 0 & \text{Cholesky}\,(R_2) & \\ & & \ddots \end{pmatrix}$$

and store the diagonal blocks of D in dblocks;

6 Let

$$U \leftarrow \begin{pmatrix} O_0 D_0^{-T} & O_1 D_1^{-T} & 0 & \cdots & 0 \\ 0 & O_2 D_1^{-T} & O_3 D_2^{-T} & & \\ 0 & 0 & O_4 D_2^{-T} & \ddots & \\ \vdots & & & \ddots & \end{pmatrix}$$

and store diagonal and upper-off-diagonal blocks of U in (fblocks,gblocks);

7 Let

$$\tilde{J} = \begin{pmatrix} R_1 & 0 & 0 \\ 0 & R_3 & \\ & & \ddots \end{pmatrix} - UU^\top$$

and store the diagonal and lower-offdiagonal blocks of $\tilde{J}$ in newrblocks,newoblocks;

8 newdlist,newflist,newglist ← decompose(newrblocks,newoblocks,len(newrblocks));

9 **return** concat([dblocks],newdlist),concat([fblocks],newflist),concat([gblocks],newglist);

10 **end**

Observe that the dlist,flist,glist returned by this algorithm stores everything we would need to reconstruct the $\text{CyclicReduction}(J)$.

How long does this algorithm take?

- Step 5 requires we compute m Cholesky decompositions
- Step 6 requires $m - 1$ triangular solves
- Step 7 has two components. First we must compute the diagonal and lower-off-diagonal blocks of $UU^\top$ (which requires about m matrix-multiplies and m matrix additions). Second we must compute $\lfloor m/2 \rfloor$ matrix subtractions.
- Step 8 requires we run the CR algorithm on a problem with $\lfloor m/2 \rfloor$ blocks.

Let $C(m)$ denote overall number of operations for a Cyclic Reduction on an m-block matrix. Since steps 7, 8, and 9 require $O(m)$ operations, we have that there exists some c such that

$$C(m) \leq cm + C(\lfloor n/2 \rfloor) \qquad C(1) \leq c$$

from which we see that $C(m) < 2cm$,[4] i.e. the computation scales linearly in m.

What about parallelization? To compute steps 5-7 we need to compute many small Cholesky decompositions, compute many small triangular solves, compute many small matrix multiplies. These are all common problems, and blazing fast algorithms exist for achieving these goals on multiple CPU cores or using GPUs.

[4] One way to see this is by induction. For the base case, we have $C(1) \leq c$. Then, under the inductive hypothesis, we have that $C(m) < c(m + 2m/2) = 2cm$. In general for all the recursive algorithms that follow, to prove linear-time it will suffice to show that the non-recursive steps require $O(m)$ time.

D.2.2 Solving $Lx = b$

This algorithm uses the tuple (dlist,flist,glist) representing a Cyclic Reduction L on a matrix with m blocks to compute $L^{-1}b$.

Algorithm 2: halfsolve

input : dlist,flist,glist,b,m
output : $x = L^{-1}b$

1 Adopt the notation D is the block-diagonal matrix whose diagonal blocks are given by dlist[0] ;
2 Adopt the notation that U is the upper didiagonal matrix whose diagonal blocks are given by flist[0] and whose upper off-diagonal blocks are given by glist[0];
3 **if** $m = 1$ **then**
4 | **return** $x = D^{-1}b$
5 **else**
6 | $x_1 \leftarrow D^{-1}P_m b$;
7 | $x_2 \leftarrow$ halfsolve(dlist[1:],flist[1:],glist[1:],$Q_m b - Ux_1$,$\lfloor m/2 \rfloor$);
8 | **return**

$$x = \begin{pmatrix} x_1 \\ x_2 \end{pmatrix}$$

9 **end**

Note that step 6 requires $O(m)$ operations, the base case requires $O(1)$ operations, and step 7 is a recursion on a problem of half-size. The overall computation thus scales linearly in m. Moreover, step 6 can be understood as m independent triangular solves, all of which can be solved completely independently (this algorithm is thus easy to parallelize across many cores).

D.2.3 Solving $L^\top x = b$

This algorithm uses the tuple (dlist,flist,glist) representing a Cyclic Reduction L on a matrix with m blocks to compute $L^{-\top}b$.

Algorithm 3: backhalfsolve

input : dlist,flist,glist,b,m
output : $x = L^{-\top}b$

1 Adopt the notation D is the block-diagonal matrix whose diagonal blocks are given by dlist[-1] (i.e. the last entry in dlist);
2 Adopt the notation that U is the upper didiagonal matrix whose diagonal blocks are given by flist[-1] and whose upper off-diagonal blocks are given by glist[-1];
3 **if** $m = 1$ **then**
4 | **return** $x = D^{-T}b$
5 **else**
6 | $\tilde{x}_2 \leftarrow$ backhalfsolve(dlist[:-1],flist[:-1],glist[:-1],b,$\lfloor m/2 \rfloor$);
7 | $\tilde{x}_1 \leftarrow D^{-\top}(P_n b - U^\top \tilde{x}_2)$;
8 | **return**

$$x = \begin{pmatrix} P_n^\top & Q_n^\top \end{pmatrix} \begin{pmatrix} \tilde{x}_1 \\ \tilde{x}_2 \end{pmatrix}$$

9 **end**

Just like the halfsolve algorithm, the cost of backhalfsolve scales linearly in m and is easy to parallelize across the m blocks.

D.2.4 Solving $Jx = b$

1. First solve $Ly = b$ using halfsolve.
2. Then solve $L^T x = y$ using backhalfsolve.

Then

$$Jx = LL^T x = Ly = b$$

as desired.

D.2.5 Computing determinants

The determinant of a block-Cholesky decomposition is just the square of the product of the determinants of the diagonal blocks. Thus if (dlist,flist,glist) represents the CR decomposition of J we have that the determinant of J is given by the square of the products of the determinants of all the matrices in dlist. This can be done in parallel across all of the m blocks, requiring $O(m)$ operations in total.

D.2.6 Computing the diagonal and off-diagonal blocks of the inverse

Algorithm 4: invblocks

input : dlist,flist,glist
output : diags,offdiags – the diagonal and off-diagonal blocks of J

1 Adopt the notation D is the block-diagonal matrix whose diagonal blocks are given by dlist[-1] (i.e. the last entry in dlist);
2 Adopt the notation that U is the upper didiagonal matrix whose diagonal blocks are given by flist[-1] and whose upper off-diagonal blocks are given by glist[-1];
3 **if** $m = 1$ **then**
4 | **return** $[D^{-T}D^{-1}]$,[]
5 **else**
6 | subd,suboff $\leftarrow$ invblocks(dlist[:-1],flist[:-1],glist[:-1]);
7 | Adopt the notation that $\tilde{\Sigma}$ is a matrix whose diagonal blocks are given by subd and whose lower off-diagonal blocks are given by suboff;
8 | Let SUDid store the diagonal blocks of $\tilde{\Sigma}UD^{-1}$;
9 | Let DitUtSo store the upper-off-diagonal blocks of $D^{-\top}U^{\top}\tilde{\Sigma}$;
10 | Let DitUtSUDid store the diagonal blocks of $D^{-\top}U^{\top}\tilde{\Sigma}UD^{-1}$;
11 | Let

$$\text{diags} \leftarrow \begin{pmatrix} P_n^{\top} & Q_n^{\top} \end{pmatrix} \begin{pmatrix} \text{DitUtSUDid} \\ \text{subd} \end{pmatrix}$$

| where DitUtSUid and subd are understood as tall columns of matrices. For example, if each block is $\ell \times \ell$, we understand DitUtSUDid as a $\lceil m/2 \rceil \times \ell$ matrix;
12 | Let

$$\text{offdiags} \leftarrow \begin{pmatrix} P_n^{\top} & Q_n^{\top} \end{pmatrix} \begin{pmatrix} \text{SUDid} \\ \text{DitUtSo} \end{pmatrix}$$

| where SUDid and DitUtSo are understood as tall columns of matrices;
13 | **return** diags,offdiags;
14 **end**

The cost of this algorithm scales linearly in m because steps 7-11 require $O(m)$ operations. To see how this can be so, recall that U is block didiagonal and D is block diagonal. Thus, for example, step 8 involves ΣUD^{-1}. Computing this entire matrix would be quite expensive. However, U is block didiagonal and we only need the diagonal blocks of the result, so we can get what we need in linear time and we only need to know the diagonal and off-diagonal blocks of Σ. As in the other algorithms, note that all of the steps can be done in parallel across the m blocks.

Why does this algorithm work? As usual, let

$$\begin{aligned} L = \text{CyclicReduction}\,(J, m) &= \begin{pmatrix} P_m^T & Q_m^T \end{pmatrix} \begin{pmatrix} D & 0 \\ U & \tilde{L} \end{pmatrix} \\ D &= \text{Cholesky}\left(P_m J P_m^{\top}\right) \\ U &= Q_m J P_m^{\top} D^{-\top} \\ \tilde{J} &= Q_m J Q_m^{\top} - U^{\top} U \\ \tilde{L} &= \text{CyclicReduction}\left(\tilde{J}, \lceil m/2 \rceil\right) \end{aligned}$$

Now let $\tilde{\Sigma} = \tilde{J}^{-1}$. It follows that

$$J^{-1} = \begin{pmatrix} P_n \\ Q_n \end{pmatrix} \begin{pmatrix} D^{-T}D^{-1} + D^{-\top}U^\top \tilde{\Sigma} U D^{-1} & -D^{-\top}U^\top \tilde{\Sigma} \\ -\tilde{\Sigma} U D^{-1} & \tilde{\Sigma} \end{pmatrix} \begin{pmatrix} P_n^T & Q_n^\top \end{pmatrix}$$

So to compute the diagonal and off-diagonal blocks of J^{-1} we just need to collect all the relevant blocks from the the inner matrix on the RHS of the equation above. Luckily, all of the relevant blocks can be calculated using only the diagonal and off-diagonal blocks of $\tilde{\Sigma}$. This is what the invblocks algorithm does.

D.3 Gradients of matrix exponentials

Above we have demonstrated linear-time algorithms for computing many useful properties of the block-tridiagonal matrices, but in order to learn LEG models via gradient descent we will also need to be able to compute gradients of these properties with respect to the parameters. Most of these gradients can be computed automatically through a package such as tensorflow

There is one gradient which standard packages will compute inefficiently. For many different values of t, we need to compute the value of $\exp(-tG)$. By default, most packages will simply compute all the matrix exponentials for each t separately, which is quite expensive. However, all these matrix exponentials can be computed much more efficiently if G is first diagonalized. On the other hand, differentiating through diagonalization isn't very stable. Thus, to get the gradients we need in a fast and stable manner we need to special-case the gradient-computation algorithm using the work of Najfeld and Havel [1995]. For the benefit of the reader we outline the relevant algorithm, below:

Algorithm 5: expm

input : G (a square matrix), tlist (a list of scalars)
output : rez (the value of $\exp(tG)$ for each t in tlist), grad (a corresponding gradient-evaluating function)

$\Lambda, U \leftarrow$ eigendecomposition(G);
$\mathrm{Ui} \leftarrow U^{-1}$;
$\mathrm{rez}_{\mathrm{mjk}} \leftarrow \sum_r U_{jr}\mathrm{Ui}_r k \exp(\Lambda_r \mathrm{tlist}_m)$;
grad $\leftarrow (M \mapsto \mathrm{expmgrad}(\Lambda, U, \mathrm{Ui}, \mathrm{rez}, M))$

Algorithm 6: expmgrad

input : G, Λ,U,Ui,rez,M,tlist
output : gradG $(mjk \mapsto \sum_{jk} M_{kr}(\partial \exp(\mathrm{tlist}_{\mathrm{m}} G)_{kr}/\partial G_{ij})$

and gradt $(m \mapsto \sum_{jk} M_{kr}(\partial \exp(tG)_{kr}/\partial t|_{t=\mathrm{tlist}_{\mathrm{m}}})$
$\Phi_{mij} \leftarrow \lim_{\lambda \to \Lambda_i}(\exp(\lambda \mathrm{tlist}_{\mathrm{m}}) - \exp(\Lambda_j \mathrm{tlist}_{\mathrm{m}})/(\lambda - \Lambda_j)$;
$H_{ij} \leftarrow \sum_m \Phi_{mij}(U^\top M_m \mathrm{Ui}^\top)_{ij}$;
$\mathrm{sand} \leftarrow \mathrm{Ui}^\top H U^\top$;
return $\Re(\mathrm{sand})$;

D.4 Learning

We are now positioned to design an algorithm to learn a LEG model from data via maximum likelihood. We need three ingredients. We describe them here:

- The ability to efficiently compute the likelihood and the gradient of the likelihood. This is facilitated by the algorithms above.
- An optimization algorithm that uses those gradients. We use BFGS, as implemented by scipy.optimize.
- Initial conditions. In the leggps package (described below) the user can provide their own initial conditions. If none are provided, we use the following simple initialization which seemed to work in practice for all the problems we looked at:
  - $N = I$. This assumes that the smoothness lengthscale of the time series is roughly on the order of one unit. If this is not the case, one can either scale the input times or provide a correspondingly different N. In general, the smoothness timescale is inversely proportional to $NN^\top$.
  - Each entry of R is sampled from $\mathcal{N}(0, \sqrt{.2})$. This assumes that the oscillations of the timeseries are roughly at a frequency of .2 oscillations per unit of time (i.e. one oscillation for every five units of time).

  - $\Lambda = .1I$. This assumes that the independent noise has a standard deviation of roughly .1.

  Even when the true smoothness lengthscale was hundreds of times different from unity, we found that BFGS was able to detect this and adjust quickly to a better regime.

This optimization problem does not appear to be convex. There were cases where we found that multiple restarts (each initialized with the same random initialization routine, described above) resulted in superior fits. The user may wish to try this if the result is unsatisfactory the first time.

When the observations are regularly spaced, a learned AR model could also be used to initialize the parameters of the LEG model, though we have not worked out exactly how this would be done. There is also a literature on using Hankel matrices to guess the dynamics of state-space models like the LEG model. In the future we hope to explore new methods for initializing. If you have ideas, don't hesitate to raise an issue on the GitHub repo.

E The leggps python package

The leggps python package can be found at `https://github.com/jacksonloper/leg-gps`. It provides functionality for working with LEG models and also exposes some of the cyclic reduction algorithms.

E.1 Working with LEG processes

leggps follows a few conventions:

- All vectors and matrices are represented as numpy objects.
- A LEG model is represented by a matrix-valued dictionary with keys for N, R, B, and Lambda.
- m observations from a LEG model comprise a sequence of times and a sequence of values.
  - The times $t_1 \leq t_2 \leq t_3 \cdots t_m$ are represented as a vector of length m. We assume these times are sorted.
  - The corresponding observations $\vec{x}$ are represented as a matrix. If the LEG process has the form $z : \mathbb{R} \to \mathbb{R}^n$, this matrix will have dimensions $m \times n$. To avoid mistakes, even if the LEG process has the form $z : \mathbb{R} \to \mathbb{R}^n$, we will expect a matrix with dimensions $m \times 1$.

  We assume that the observations of x arise from a LEG model, i.e. $z \sim \mathrm{PEG}(N, R)$ and

  $$\vec{x}_i \sim \mathcal{N}(Bz(t_i), \Lambda\Lambda^\top)$$

  Note that if $t_i = t_i + 1$ we assume that $\vec{x}_i, \vec{x}_{i+1}$ are sampled independently.
- Sometimes we will wish to represent several independent samples from a LEG model. For example, perhaps each independent sample represents a neural recording on a different day. We will represent this using a list of time-vectors and a corresponding list of observation matrices. That is, we will have that
  - ts[i][j] indicates the time of the jth observation in the ith independent sample
  - xs[i][j,k] indicates the kth dimension of the jth observation in the ith independent sample

leggps provide the following functions:

leggps.C_LEG Calculates the covariance of a LEG process for various values of τ. Inputs:

taus A vector of m times, $\tau_1 \leq \tau_2 \leq \tau_3 \cdots$

N,R,B,Lambda Model parameters

Outputs an $m \times n \times n$ tensor. The ith element of this indicates indicates $C_{\mathrm{LEG}}(\tau_i; N, R, B, \Lambda)$.

leggps.leg_log_likelihood Calculates the log likelihood of an observation under a LEG model.

Inputs:

ts A vector of m times, $t_1 \leq t_2 \leq t_3 \cdots t_m$

xs A matrix of observations at those times, i.e. $\vec{x} = x(t_1), x(t_2), \cdots$.

N,R,B,Lambda Model parameters

Outputs the log likelihood.

leggps.leg_log_likelihood_tensorflow Essentially the same as the function above, but inputs and outputs are assumed to be TensorFlow2 objects. This may be helpful if you would like to efficiently calculate gradients, write your own optimization routines, or use the LEG family as a building block in a larger model (e.g. one can put a prior on the parameters and use the gradient together with Hamiltonian Monte-Carlo to sample from the posterior on the parameters N, R, B, Λ). To make this fast, we recommend enclosing your code with a tf.function(autograph=False) decorator, compiling the operations to a graph which can be run quite efficiently.

Inputs:

ts A vector of $\tilde{m}$ times, $t_0 < t_1 < t_2 \cdots t_{\tilde{m}-1}$. Note that these times *must* be distinct (compare with the leg_log_likelihood which allows non-distinct values).

xs A matrix of m observations, each of which was taken at one of those times. In particular, $\vec{x} = x(t_{\texttt{idxs}_0}), x(t_{\texttt{idxs}_1}), \cdots$, where...

idxs is a vector of length m indicating which observations came from which times. Each entry of idxs should be an integer in the set $\{0, 1, \cdots \tilde{m} - 1\}$.

N,R,B,Lambda Model parameters

This function does enable computation with multiple observations taken at the same time (and assumes they are independently sampled) – but the user must ensure that the vector of times contains no duplicates and the user must figure out which observations correspond to what entry of that time-vector. Compare with the function leg_log_likelihood: the non-TensorFlow2 function isn't designed for speed, so it does this deduplication automatically at every invocation.

Outputs the log likelihood.

leggps.posterior_predictive Indicates interpolations/forecasts, i.e $BE[z(t)|\vec{x}]$ and $B\mathrm{Cov}(z(t)|\vec{x})B^\top$ for various values of t.

Inputs:

ts A vector of m times, $t_1 \leq t_2 \leq t_3 \cdots t_m$

x A matrix of observations at those times, i.e. $\vec{x} = x(t_1), x(t_2), \cdots$.

targets A vector of times at which to evaluate the interpolations/forecasts, based on the data $\vec{t}, \vec{x}$.

N,R,B,Lambda Model parameters

Outputs a tuple with two elements:

1. Means, a matrix indicating $BE[z(\texttt{targets}_i)|\vec{x}]$
2. Variances, n $m \times n \times n$ tensor. The ith element of this indicates $B\mathrm{Cov}(z(\texttt{targets}_i)|\vec{x})B^\top$

leggps.posterior Indicates posterior moments, i.e $E[z(t)|\vec{x}]$ and $\mathrm{Cov}(z(t)|\vec{x})$ for various values of t.

Inputs:

ts A vector of m times, $t_1 \leq t_2 \leq t_3 \cdots t_m$

x A matrix of observations at those times, i.e. $\vec{x} = x(t_1), x(t_2), \cdots$.

targets A vector of times at which to evaluate the interpolations/forecasts, based on the data $\vec{t}, \vec{x}$.

N,R,B,Lambda Model parameters

Outputs a tuple with two elements:

1. Means, a matrix indicating $E[z(\texttt{targets}_i)|\vec{x}]$
2. Variances, n $m \times n \times n$ tensor. The ith element of this indicates $\mathrm{Cov}(z(\texttt{targets}_i)|\vec{x})$

leggps.fit uses a collection of independent samples to learn a LEG model. For each sample i we assume that

$$t_{i1} \leq t_{i2} \leq t_{i2} \cdots \leq t_{i,m_i}$$
$$z_i \sim \mathrm{PEG}(N, R) \qquad x_i(t)|z \sim \mathcal{N}(Bz_i(t), \Lambda\Lambda^\top)$$
$$\vec{x}_i = (x_i(t_{i1}), x_i(t_{i2}), x_i(t_{i3}), \cdots)$$

If the process is of the form $x : \mathbb{R} \to \mathbb{R}^n$ we expect each $\vec{x}_i$ to be an $m_i \times n$ matrix. Even if x is a process $x : \mathbb{R} \to \mathbb{R}^1$, we expect each $\vec{x}_i$ to be a $m_i \times 1$ matrix.

We attempt to maximize the likelihood of this data with respect to N, R, B, Λ.

Inputs:

ts a list of vectors of timepoints. The ith entry in this list is itself a vector of times, $t_{i1} \leq t_{i2} \leq t_{i2} \cdots$.

xs a list of observation matrices. The ith entry in this list corresponds to the matrix $\vec{x}_i \in \mathbb{R}^{m_i \times n}$.

ell the rank of the LEG model to be learned

N,R,B,Lambda initial conditions (otherwise will be randomly initialized)

maxiter=200 maximum number of iterations of BFGS to use

use_tqdm_notebook=False if True, uses tqdm.notebook to display training progress

diag_Lambda=False if True, enforces that Lambda is a diagonal matrix (can be essential if n is large)

Output is a dictionary with many keys. Perhaps the most important keys is "params," which corresponds to the learned parameters, but there are many others which give useful information about the optimization process used to find those parameters:

params A dictionary indicating the learned parameters. It contains four elements: N, R, B, and Lambda, corresponding to N, R, B, Λ.

fun The nats at completion of the optimization

jac The gradient at completion of the optimization

hess_inv The estimate of the inverse of the hessian at completion of the optimization

nfev The number of times the likelihood was evaluated

njev The number of times the gradient of the likelihood was evaluated

status A status code (see scipy.optimize.minimize for details)

success Whether we were able to find a local optimum (up to machine precision). In practice, this usually is not true; nonetheless the learned parameter values perform well.

message A message indicating under what conditions the optimization terminated

nit The number of iterations used by the optimization algorithm

losses A list of the nats discovered along the optimization process. Note that the final loss may not be the same as the nats for the learned params – BFGS always picks the best parameter values that it found, which may not be the last parameter values it looked at.

E.2 Working with Cyclic Reductions

The leggps package also exposes an API for cyclic reduction algorithms.

This API is more low-level. All inputs are assumed to be TensorFlow2 objects and the outputs are likewise TensorFlow2 objects. Most of the functions in this package should be run on the CPU not the GPU, because the CUDA implementations for Cholesky decomposition and triangular_solve are currently still quite bad for handling many decompositions at once (as of this writing, 2020). The m5 line of machines in the AWS platform is fairly cost-effective for running these functions on the CPU.

This package follows the convention that block-tridiagonal matrices are represented as (Rs,Os) where Rs indicates the block diagonal components and Os indicates the lower off-diagonal blocks. Thus Rs will be an $m \times \ell \times \ell$ tensor and Os will be an $m - 1 \times \ell \times \ell$ tensor. We assume all the blocks are the same size.

leggps provides the following functions:

leggps.cr.decompose(Rs,Os) Let J denote the block-tridiagonal matrix represented by Rs,Os. This function returns an opaque representation of the CR decomposition of the block-tridiagonal matrix. This can be used in other functions.

leggps.cr.mahal(decomp,x) Let J denote the block-tridiagonal matrix whose CR decomposition is given by decomp. Evaluates $x^T J^{-1} x$.

leggps.cr.det(decomp) Let J denote the block-tridiagonal matrix whose CR decomposition is given by decomp. Evaluates the log determinant of J.

leggps.cr.mahal_and_det(Rs,Os,x) Let J denote the block-tridiagonal matrix represented by Rs,Os. Uses CR algorithms to to evaluate $x^T J^{-1} x$ and compute the log determinant of J. This function may require half as much RAM than using the functions above – it never stores the entire decomposition at once.

leggps.cr.solve(decomp,y) Let J denote the block-tridiagonal matrix whose CR decomposition is given by decomp. Returns $J^{-1} x$.

leggps.cr.sample(decomp) Let J denote the block-tridiagonal matrix whose CR decomposition is given by decomp. Samples from $\mathcal{N}(0, J^{-1})$.

leggps.cr.inverse_blocks(decomp) Let J denote the block-tridiagonal matrix whose CR decomposition is given by decomp. Returns the diagonal and off-diagonal blocks of J^{-1}.

F Extensions

There are a number of ways this package could be extended if there was sufficient interest. Raise an issue on the GitHub repo if these or other extensions would be important to your work.

Some extensions we have considered:

- We assume each observation is always fully observed, i.e. if we observe $x(t_i) \in \mathbb{R}^n$ then we observe all n numbers. This restriction could be lifted.
- The CR algorithms assume all blocks are the same size. If you need the blocks need to be of different sizes the TensorFlow2 raggedtensor API could conceivably be used to lift this limitation.
- We assume the noise variance, Λ, is the same for each observation. It would be fairly straightforward to lift this restriction.
- The observations do not need to lie along a line – in general, they could lie along any one-dimensional tree-structured topology.
- The model does not need to be stationary. If there are specific nonstationarities you would like to capture, the authors would be interested in discussing them with you and figuring out which (of many possible) options would be most useful in incorporating nonstationarity.
- We would like to think about better initialization strategies. If you are having difficulty initializing the LEG model for a scientific problem, the authors would be interested in discussing your problem and thinking about what might work.

There are also two extensions we have considered in some depth. We detail these below.

F.1 Multi-dimensional GPs

Let $z: \mathbb{R}^d \to \mathbb{R}^n$ denote a Gaussian Process with covariance kernel

$$\Sigma: \mathbb{R}^d \to \mathbb{R}^{n\times n}$$

How can we use LEG kernels could be used to model Σ? One technique to build one-dimensional models into multi-dimensional models is by using Kronecker products [Tsiligkaridis and Hero, 2013]. Here we generalize this to processes with $n > 1$.

Definition 10. For each $k \in 1 \cdots d$, let $C_k: \mathbb{R} \to \mathbb{R}^{\ell\times\ell}$ denote integrable continuous kernels. If $C: \mathbb{R}^d \to \mathbb{R}^{n\times n}$ is given by

$$C_{ij}(\tau) = \prod_k C_{kij}(\tau_k)$$

then we will say C is the **Kronecker-Hadamard product** of $C_1, C_2 \cdots C_d$, and write $C = \circledast_{k=1}^d C_k$.

Proposition 6. *Let $C_1, C_2 \cdots C_d$ denote integrable continuous positive-definite kernels. Then $C = \circledast_k^d C_k$ is also positive definite.*

Proof. Let M_k denote the spectrum of C_k. Recall that M_k is a positive-definite-matrix-valued function. Let $M_{ij}(\omega) = \prod_k M_{kij}(\omega)$. Observe that M is the spectrum of C. On the other hand, the Schur product theorem shows that $M(\omega)$ is a positive definite matrix. Bochner's theorem then yields that C is positive definite. □

We can combine PEG kernels via these Kronecker-Hadamard products, leading to a multidimensional extension to LEG models.

Definition 11. Fix ℓ, ζ. For each $r \in \{1 \cdots \zeta\}, k \in \{1 \cdots d\}$, let N_{rk}, R_{rk} be $\ell \times \ell$ matrices. Consider the kernel defined by

$$C_{\mathrm{KPEG}}(N, R, B, \Lambda) \triangleq \sum_{r=1}^{\zeta} \circledast_{k=1}^d C_{\mathrm{PEG}}(N_{rk}, R_{rk})$$

We will call this the Kroneckered Purely Exponentially Generated (KPEG) kernel. If z is a zero-mean Gaussian Process whose covariance is a KPEG kernel we will say it is a KPEG process. Furthermore, let $B \in \mathbb{R}^{n\times\ell}, \Lambda \in \mathbb{R}^{n\times n}$. If z is a KPEG process and $x(\tau)|z \sim \mathcal{N}(Bz(\tau), \Lambda\Lambda^\top)$ we will say x is a KLEG process. We will call the covariance kernel of x a KLEG kernel, denoted $C_{\mathrm{KLEG}}(N, R, B, \Lambda)$.

Theorem 3. *Let Σ any positive-definite integrable continuous kernel, and fix $\varepsilon > 0$. There exists a KLEG kernel such that $\|C(\tau)z - C_{\mathrm{KLEG}}(\tau)z\| < \varepsilon z$.*

Proof. The proof is essentially the same as that of Theorem 2. Note the spectrum of a C_{KLEG} kernel can be understood as a mixture of matrix-valued densities on $\mathbb{R}^d$, and the N, R parameters can be used to arbitrarily shift and scale these spectral densities. Applying Theorem 1, it follows that we can match every element of any spectrum arbitrarily well in an integrated-absolute-value-sense using KPEG kernels. It follows that we can match any integrable continuous positive-definite kernel in a uniform sense. □

We can compute efficiently with such kernels if the observations are taken on a d-dimensional grid. For example, GPyTorch offers algorithms for Gaussian processes where the runtime is limited only by the speed with which one can multiply by the covariance matrix [Gardner et al., 2018]. If we have observations from a KPEG model on a grid, this can be done efficiently:

Theorem 4. *Let $\Omega = \prod_k^d \{\tau_{k1}, \tau_{k2} \cdots \tau_{km}\} \subset \mathbb{R}^d$ denote a grid. Let x denote a KLEG process and let $\vec{x}$ denote observations of x on this grid. Let Σ denote the covariance matrix of $\vec{x}$ under the KLEG model. For any y the time required to compute Σy scales like m^d. In particular, in the limiting case where we have an observation at each grid-point, we have m^d observations and the computation scales linearly in the number of observations.*

Proof. It suffices to show that we can perform matrix-multiplications in m^d time for matrices which are the Kronecker-Hadamard product of d matrices when the inverses of those matrices are block-tridiagonal with m blocks of size ℓ. It suffices to show for the case $d = 2$ and apply induction.

Let C, D denote block-tridiagonal matrices. We will index them by $C_{i,j}(\tau_{1s}, \tau_{1s'})$ and $D_{i,j}(\tau_{2u}, \tau_{2u'})$. Because D^{-1} is block-tridiagonal, we can compute Dy in linear time. That is, we can compute

$$(Dy)_{i,u} = \sum_{j=1}^{\ell} \sum_{u'=1}^{m} D_{i,j}(\tau_{2u}, \tau_{2u'}) y_j(\tau_{2u'})$$

in $O(m)$ steps. It follows we can also compute

$$\xi_{i,j,u} = \sum_{u'} D_{i,j}(\tau_{2u}, \tau_{2u'}) y_j(\tau_{2u'})$$

in $O(m)$ steps (for each j, define $\tilde{y}$ by $\tilde{y}_{j'} = \delta_{j,j'} y_{j'}$, then $\xi_{i,j,u} = D\tilde{y}$).

We are interested in the Kronecker, i.e.

$$F_{i,j}(\tau_{1s}, \tau_{2u}, \tau_{1s'}, \tau_{2u'}) = C_{i,j}(\tau_{1s}, \tau_{1s'}) D_{i,j}(\tau_{2u}, \tau_{2u'})$$

Given an observation y we need to compute

$$\begin{aligned}(Fy)_i(\tau_{1s}, \tau_{2u}) &= \sum_{j,s',u'} F_{i,j}(\tau_{1s}, \tau_{2u}, \tau_{1s'}, \tau_{2u'}) y_j(\tau_{1s'}, \tau_{2u'}) \\ &= \sum_{j,s'} C_{i,j}(\tau_{1s}, \tau_{1s'}) \underbrace{\sum_{u'} D_{i,j}(\tau_{2u}, \tau_{2u'}) y_j(\tau_{1s'}, \tau_{2u'})}_{\triangleq \xi_{ijus'}}\end{aligned}$$

As discussed earlier, we can compute $\xi_{ijus'}$ independently for each s' in $O(m)$ time; the total computation time will be $O(m^2)$. Once this is computed, we can compute $(Fy)(\cdot, \tau_{2u})$ in $O(m)$ time for each u – an overall cost of $O(m^2)$. The result is that the total computation requires $O(m^2)$ operations, as desired.

□

Combining the previous two propositions, we see that arbitrarily accurate linear-time inference is possible for any Gaussian Process as long as we observe the process on a multidimensional grid. Note that this grid does not need to be regularly spaced. Moreover, it is straightforward to see that we do not need to have observations from every point in the grid. However, note that the computational cost will scale with the number of gridpoints (not the number of observations). In particular, if our observations occur on a very small proportion of the gridpoints, then different methods may be required.

F.2 Non-Gaussian observations

Many approaches have been developed to adapt GP inference methods to non-Gaussian observations, including Laplace approximations, expectation propagation, variational inference, and a variety of specialized Monte Carlo methods [Hartikainen et al., 2011, Riihimäki et al., 2014, Nguyen and Bonilla, 2014, Nishihara et al., 2014]. Many of these can be easily adapted to the LEG model, using the fact that the sum of a block-tridiagonal matrix (from the precision matrix of the LEG prior evaluated at the sampled data points) plus a diagonal matrix (contributed by the likelihood term of each observed data point) is again block-tridiagonal, leading to linear-time updates [Smith and Brown, 2003, Paninski et al., 2010, Fahrmeir and Tutz, 2013, Polson et al., 2013, Khan and Lin, 2017, Nickisch et al., 2018].

Here we sketch one way this can be achieved.

Definition 12. Let $p(x;\theta,\gamma)$ denote a family of densities indexed by $\theta \in \mathbb{R}^n$ and additional hyperparameters γ. Let $B \in \mathbb{R}^{n\times\ell}$ and $z \sim \mathrm{PEG}(N,R)$. Let $x(t)|z \sim p(Bz(t))$, independently for each t. Then we will say that x is the **Non-Gaussian Latent Exponentially Generated** (NGLEG) model parameterized by p, N, R, B.

How can we learn N, R, B, θ, γ from data? Let us say we have $t_1 < t_2 \cdots t_m$ and we have observed $\vec{x} = (x(t_1) \cdots x(t_m)$ from a NGLEG model. We adopt a Variational Inference point of view. Let $\vec{z} = (z(t_1), z(t_2), \cdots z(t_m))$. Let $\Sigma(N,R)$ denote the prior covariance of $\vec{z}$ when $z \sim \mathrm{PEG}(N,R)$. We posit a family of possible posterior distributions for $\vec{z}$, namely

$$\vec{z} \sim q(z;\mu,J) \triangleq \mathcal{N}(z;\mu,J^{-1})$$

where J is a block-tridiagonal matrix. We then seek to maximize a lower bound on the likelihood of the observations, namely

$$\begin{aligned}
\mathcal{L}(N,R,B,\gamma,J,\mu) &= \mathcal{L}_{\mathrm{data}}(B,\gamma,J,\mu) + \mathcal{L}_{\mathrm{KL}}(N,R,J,\mu) \\
\mathcal{L}_{\mathrm{data}}(B,\gamma,J,\mu) &= \sum_i \mathbb{E}_{\vec{z}\sim q}\left[\log p(\vec{x}_i; B\vec{z}_i, \gamma)\right] \\
\mathcal{L}_{\mathrm{KL}}(N,R,J,\mu) &= \frac{1}{2}\mathbb{E}_{\vec{z}\sim q}\left[-\vec{z}^\top \Sigma(N,R)^{-1}\vec{z} - \log|\Sigma(N,R)||J| + (\vec{z}-\mu)^\top J(\vec{z}-\mu)\right]
\end{aligned}$$

We refer the reader to [Blei et al., 2017] for a proof that this is indeed a lower-bound on the likelihood of $\vec{x}$. Note that $\mathcal{L}_{\mathrm{KL}}$ and its gradients can be computed in $O(m)$ time using Cyclic Reduction algorithms. For the data term we can either use Monte-Carlo samples from $\vec{z} \sim q$ or reduce the expectation to something which can be computed in terms of the mean and variance of $\vec{z}$. The Laplace method is an example of the latter approach, approximating the log likelihoods by taking a second order taylor expansion of $z_i \mapsto \log p(\vec{x}_i; B\vec{z}_i, \gamma)$ around the μ_i. The Polya-Gamma trick is another example of this method which works for Bernoulli and Negative Binomial likelihoods; this trick yields a lower-bound which can be computed in terms of the mean and variance of $\vec{z}_i$ [Polson et al., 2013]. Regardless of which approach we use for the data term, we ultimately obtain approximate gradients of $\mathcal{L}$ with respect to N, R, B, γ, J, μ and use these gradients to optimize the parameters.